

Chapter 2

Theory and Review of Literature

2.1 Fatigue of metals

2.1.1 Introduction to fatigue

Metals and alloys subjected to repetitive or fluctuating stresses fail at a stress level much lower than that required for failure on a single application of the load [2.1]. Failures occurring under such cyclic loading conditions are termed as fatigue failures. Fatigue is thus a progressive, localized, and permanent structural change that occurs in a material subjected to repeated or fluctuating strains at nominal stresses that have maximum values less than the static yield strength of the material [2.2]. There are many ways to define a fatigue failure [2.3, 2.4]. However, the one as per ASTM E206-62T states that "fatigue is the process of progressive localized permanent structural change occurring in a material subjected to conditions, which produce fluctuating stresses and strains at some point or points and which may culminate in cracks or complete fracture after a sufficient number of fluctuations"[2.5].

The majority of engineering components such as shafts, axles, gears, connecting rods, etc. are subjected to fluctuating or cyclic loads. Such loading induces fluctuating or cyclic stresses that often result in failure. Fatigue accounts for about 90% of all service failures. The damage caused during the fatigue process is cumulative and generally unrecoverable. Thorough understanding of fatigue behaviour is therefore essential for components subjected to constant variable amplitude loading.

Fatigue can be classified in two ways viz. classification on the basis of load and that on the basis of environment. On the basis of load, fatigue can be divided into two types: High Cycle Fatigue (HCF) and Low Cycle Fatigue (LCF). When the stress level is low and the deformation is primarily elastic, the fatigue is called as high cycle type. Number of cycles needed for fracture in this type is high. Also the slip bands in HCF are fine. On the other hand, when the stress level is high enough for plastic deformation to occur, the fatigue is known as low cycle type. Strain hardening can occur in LCF and the slip band produced are coarse [2.6]. Number of cycles needed for fracture in such a

case is low. Although there is no distinction or clear-cut line of demarcation between the two, the traditional approach is to classify failures occurring above 10^5 cycles as HCF and those below that value as LCF [2.7].

On the basis of environment, the different types of fatigue failure are corrosion fatigue, thermal fatigue, etc. The fatigue characteristics are affected by operating temperature and aqueous and corrosive environments.

2.1.2 History of metal fatigue

Preliminary understanding about fatigue failure of metals developed in 19th century during industrial revolution in Europe when heavy duty locomotives, boilers, etc. failed under cyclic loads. It was William Albert who in 1837 first published an article on fatigue that established a correlation between cyclic load and durability of the metal [2.8]. Two years later in 1839, Jean-Victor Poncelet, designer of cast iron axles for mill wheels, officially used the term *fatigue* for the first time in a book on mechanics. Some pioneering work followed from August Wöhler during 1860-1870 [2.1] when he investigated failure mechanism of locomotive axles by applying controlled load cycles. He introduced the concept of rotating-bending fatigue test that subsequently led to the development of stress-Number of cycles (S-N) diagram for estimating fatigue life and endurance or fatigue limit of metal, the fatigue limit representing the stress level below which the component would have infinite or very high fatigue life. By the end of 19th century, Gerber and Goodman investigated the influence of mean stress on fatigue parameters and proposed simplified theories for fatigue life. Based on these theories, designers and engineers started to implement fatigue analysis in product development and were able to predict product life better than ever before. At the beginning of the 20th century, J. A. Ewing demonstrated the origin of fatigue failure in microscopic cracks. In 1910, O.H. Baskin defined the shape of a typical S-N curve by using Wöhler's test data and proposed a log-log relationship. Birth of fracture mechanics took place with the work of Alan A. Griffith in 1920 who investigated cracks in brittle glass [2.9]. This promoted understanding of fatigue since concepts of fracture mechanics are essentially involved in fatigue crack characteristics. However, despite these developments, fatigue and fracture analysis was still not regularly practiced or implemented by the designers. Importance of the subject was finally realized when serious accidents took place around World War II in 20th century that spurred full-fledged research work on the subject.

2.1.3 Mechanism of fatigue

Metals when subjected to repeated cyclic load exhibit damage by fatigue. The magnitude of stress in each cycle is not sufficient to cause failure with a single cycle. Large number of cycles are therefore needed for failure by fatigue. Fatigue manifests in the form of initiation or nucleation of a crack followed by its growth till the critical crack size of the parent metal under the operating load is reached leading to rupture.

Entire process of failure of a component due to fatigue may be divided into three stages namely, crack initiation, crack propagation or crack growth and the stage of final fracture as displayed in the following block diagram.

Various stages of the fatigue life of a component are displayed in Figure 2.1 below.

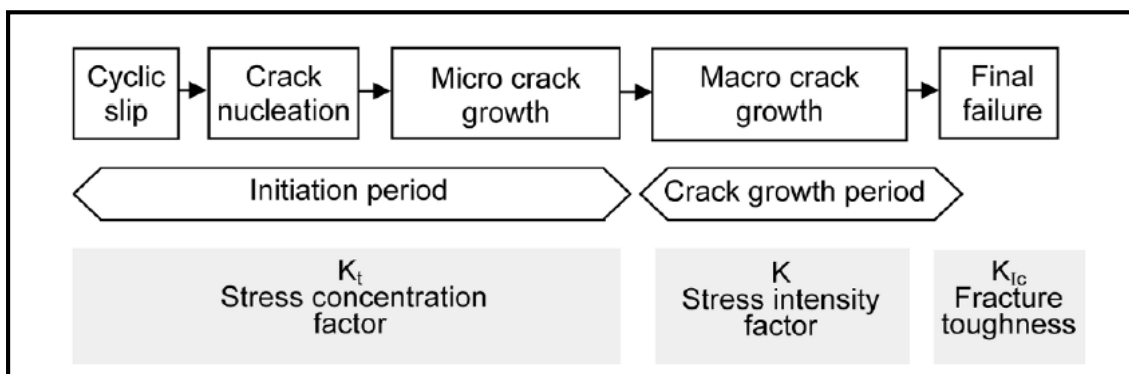


Fig. 2.1: Different phases of the fatigue life of a component and factors governing them [2.10]

Crack initiation

Fatigue failure starts even prior to initiation of a crack. Initially, with repeated loading, localized regions of slip (plastic deformation) develop. A series of intrusions and extrusions are formed on the surface of the component during the stress cycling. The slip occurs at the free surfaces as a step caused by the displacement of metal along a slip plane. When the stress is reversed, the slip that occurs is expected to be the exact negative of the original slip, completely overriding any deformation effects. However, it does not happen so and hence finally some residual deformation remains. This deformation is further accentuated by repeated loading, until a discernible crack finally appears. The entire sequence of these events has been explained in Fig.2.2 (a) to (e) while Fig. 2.3 shows the SEM image of slip lines for steel material.

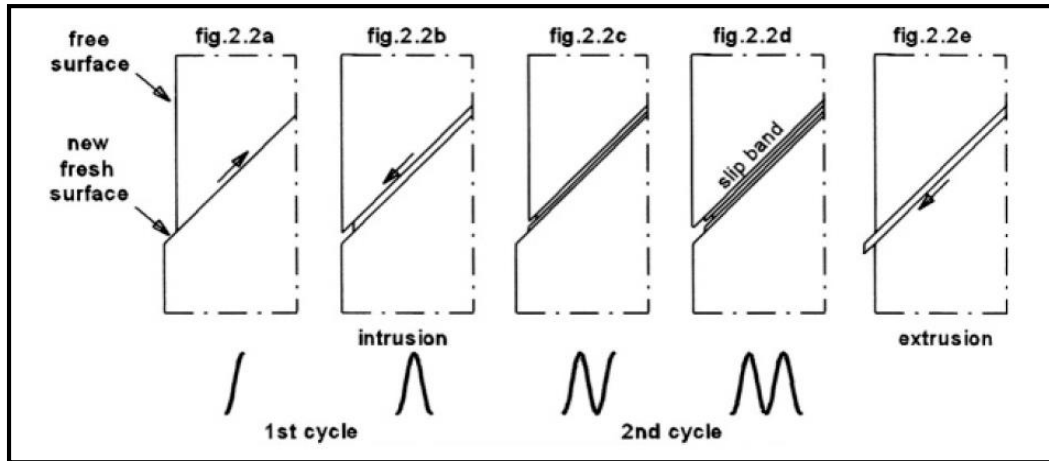


Fig. 2.2: Schematic of cyclic slip process during crack nucleation [2.10]

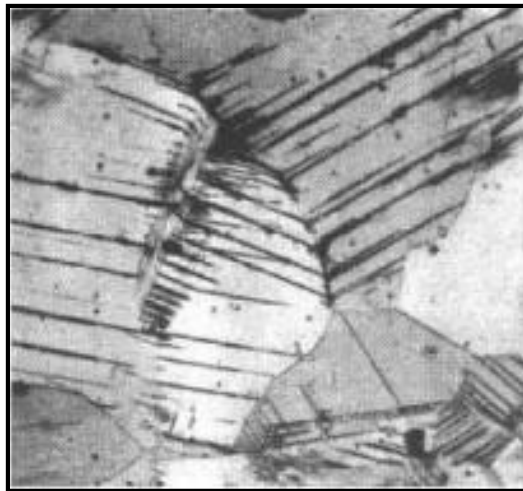


Fig. 2.3: SEM image showing slip lines [2.11]

It is worth noting that not all fatigue cracks nucleate along slip bands, although in many cases slip bands are at least indirectly responsible for micro-cracks forming in metals. For instance, fatigue cracks may nucleate at or near material discontinuities such as inclusions, second-phase particles, corrosion pits, grain boundaries, twin boundaries, pores, voids, and slip bands or sometimes just below the metal surface.

Crack propagation or crack growth

Once a micro-crack or micro-cracks are present and cycling continues, fatigue cracks tend to coalesce and grow along the plane of maximum tensile stress range. The two stages of fatigue crack growth are called "stage I" (shear mode) and "stage II" (tensile mode). Fatigue crack growth is shown schematically as a microscopic edge view in Fig. 2.4. A fatigue crack is shown to nucleate at the surface and grow across several grains, controlled primarily by shear stresses and shear strains, and then to grow in a zigzag manner

essentially perpendicular to, and controlled primarily by, the maximum tensile stress range. Most fatigue cracks grow across grain boundaries (transcrystalline). However, they may also grow along grain boundaries (intercrystalline), depending on the material, load, and environmental conditions [2.9]. Usually the crack is growing perpendicular to the main principal stress. For uniaxial loading conditions in symmetric specimens, it implies that the crack growth direction is macroscopically perpendicular to the loading direction.

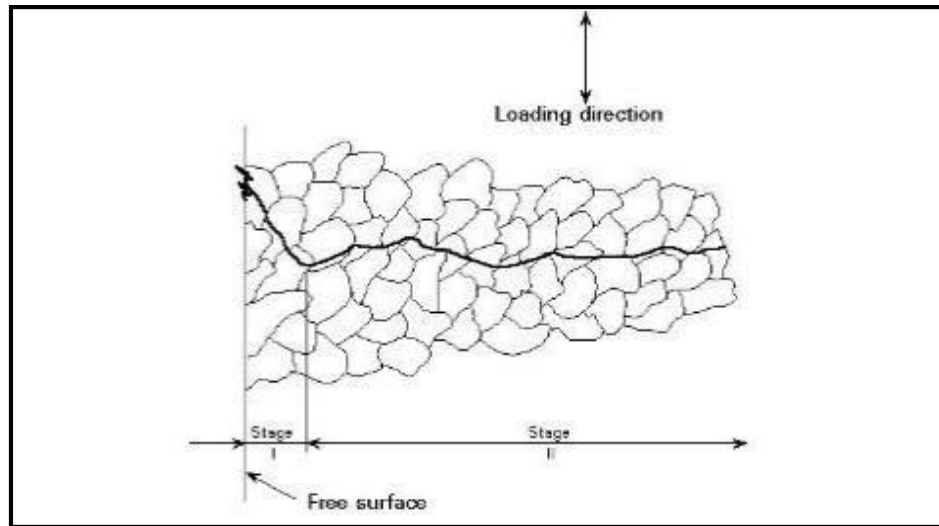


Fig. 2.4: Stage I and stage II crack growth in a polycrystalline material. Crack is growing perpendicular to the principal stress axis. [2.9]

Final fracture

Final fracture does not occur by a fatigue mechanism at all but is simply fracture caused by the last load application, resulting in complete separation. Final fracture occurs when the crack has grown to the critical size for overload failure. The size of the final-fracture zone depends on the magnitude of the loads, and its shape depends on the shape, size, and direction of loading of the fractured part. The final-fracture zone of a fatigue-fracture surface is often fibrous, resembling the fracture surfaces of impact or fracture-toughness test specimens of the same material.

2.1.4 Macro and microscopic features of fatigue

A fatigue failure has an appearance similar to a brittle fracture, as the fracture surfaces are flat and perpendicular to the stress axis with the absence of necking. The fracture features of a fatigue failure, however, are quite different from a static brittle fracture arising from three stages of development [2.10].

Stage I is the initiation of one or more micro-cracks due to cyclic plastic deformation followed by crystallographic propagation extending from two to five grains about the origin. Stage I cracks are not normally discernible to the naked eye.

Stage II progresses from micro-cracks to macro-cracks forming parallel plateau-like fracture surfaces separated by longitudinal ridges. The plateaus are generally smooth and normal to the direction of maximum tensile stress.

Stage III occurs during the final stress cycle when the remaining material cannot support the loads, resulting in a sudden fracture.

A stage III fracture can be brittle, ductile, or a combination of both. Quite often the beach marks, if they exist, and possible patterns in the stage III fracture called chevron lines, point toward the origins of the initial cracks.

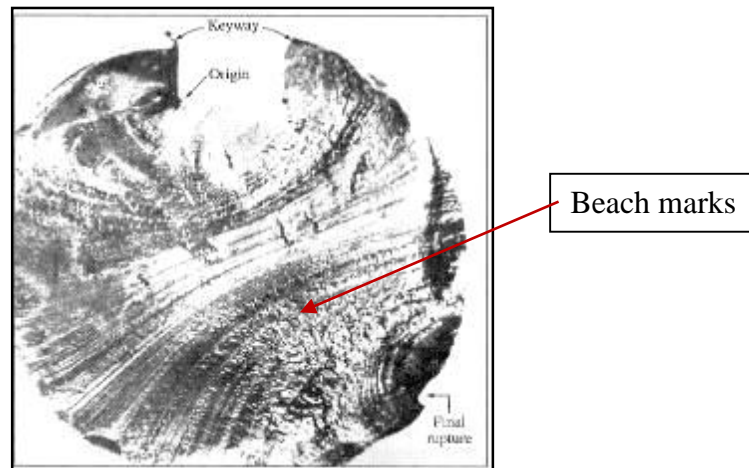


Fig. 2.5: Fracture surface of a failed shaft showing beach marks emerging from two different origins located diametrically opposite [2.11]

The surface having fractured by fatigue is characterized by two types of markings termed as beach marks and striations [2.12, 2.13]. Both these features indicate the position of the crack tip at some point of time and appear as concentric ridges that expand away from the crack initiation site frequently in a circular or semicircular pattern. Beach marks are of macroscopic dimensions as represented in Fig. 2.5, and may be observed with unaided eye. They are normally evident as somewhat wavy darker and lighter bands in the main fatigue region. The "beach marks" are also known as "clam shell markings," "arrest lines," or "conchoidal marks." However, beach marks is the most widely used term and has arisen because of the similarity of the fracture pattern to sand markings left when a wave of water leaves a sandy beach. These markings are due to the two adjacent crack surfaces that open, close, and rub together during cyclic loading, and to the crack's starting and stopping and growing at different rates during the variable (or random) loading spectrum. These markings are found in components that experience interrupted crack propagation. Each beach mark band represents a period of time over which the crack growth occurs.

On the other hand, fatigue striations are microscopic in size (Fig. 2.6) and can be viewed with an electron microscope. A striation forms a part of beach mark and represents the distance by which the crack advances during the single load cycle. The striations can give information about the crack growth direction and crack growth rate. Striation width increases with increasing stress range and vice-versa. Although both beach marks and striations have similar appearances, they are nevertheless different, both in origin and size. There may be literally thousands of striations within a single beach mark. Presence of beach marks and striations on a fractured surface confirms fatigue as the cause of failure. At the same time, absence of either or both does not exclude fatigue as the cause of failure [2.10].

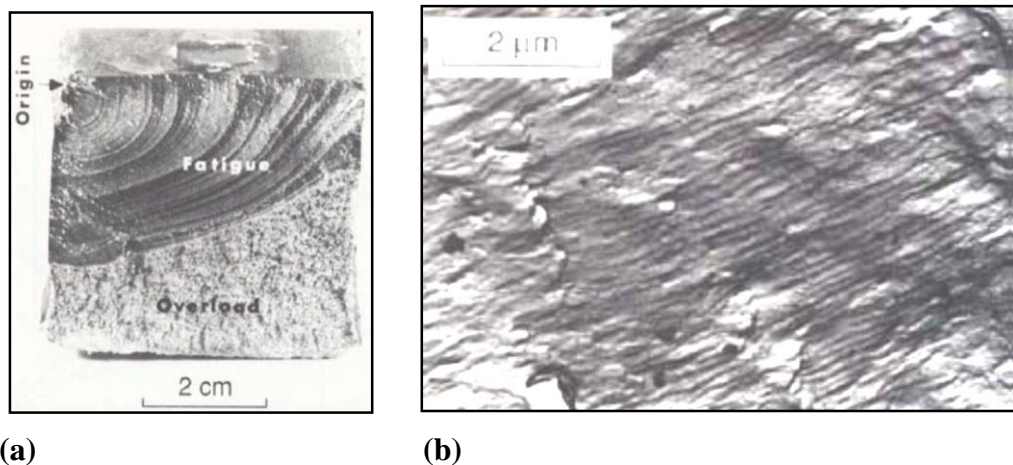


Fig.2.6: Fracture surface showing (a) macroscopic features (beach marks) and (b) microscopic features (striations) [2.16]

Figure 2.7 below gives the typical SEM fractographs for grade 42CrMo4 steel for fracture under low cycle fatigue and fracture under high cycle fatigue conditions, respectively.

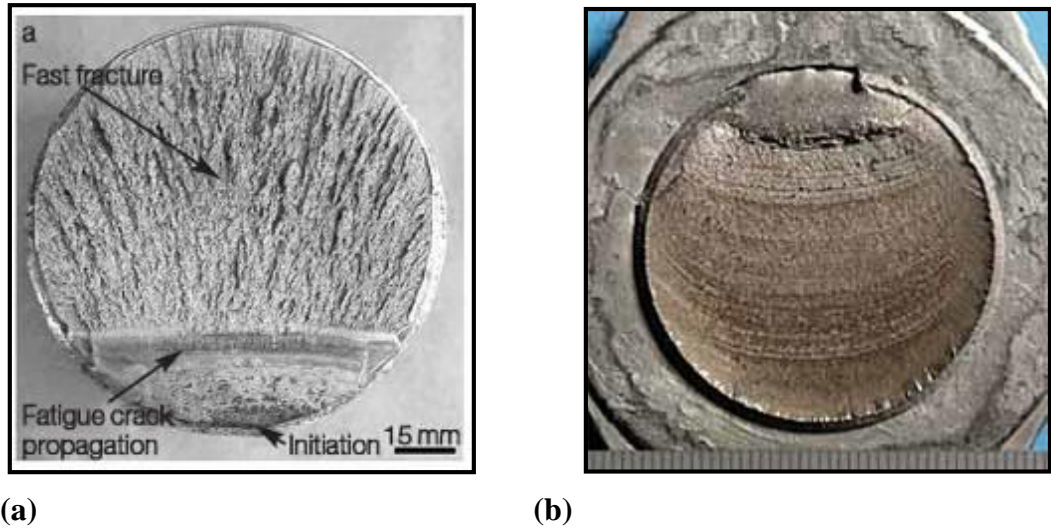
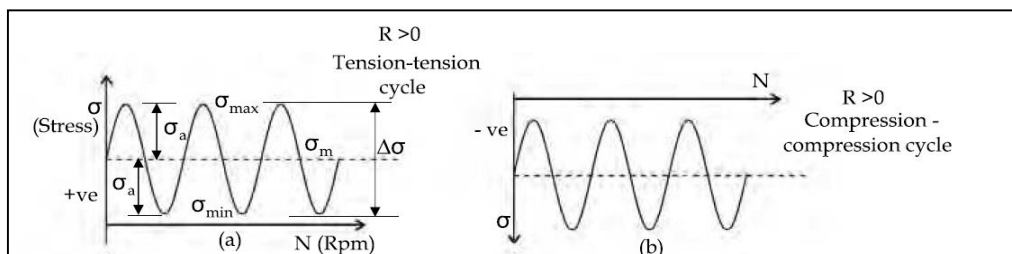


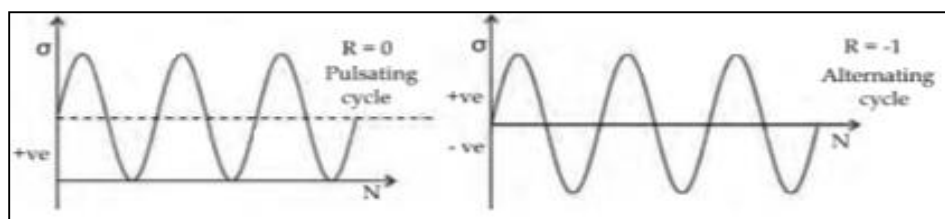
Fig. 2.7: SEM fractographs for grade 42CrMo4 steel showing: (a) Fracture surface of specimen failed under low cycle fatigue and (b) Fracture surface of the specimen failed under high cycle fatigue conditions[2.14]

2.1.5 Types of fatigue loading

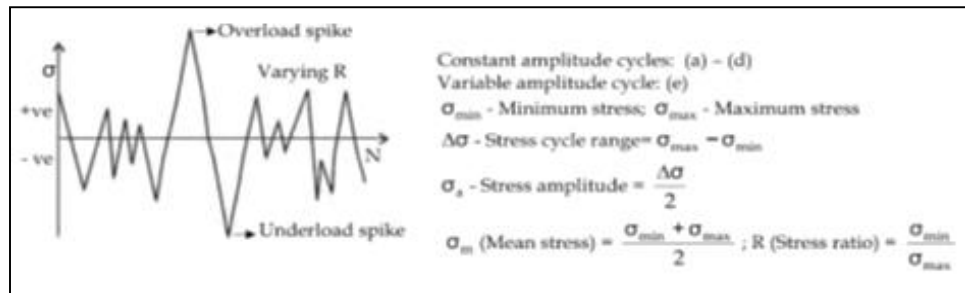
There are three types of stress cycling or loading as shown in Figure 2.8 along with the different terminologies used. They are: (i) complete reversal, (ii) repeated and (iii) the random or complicated. In complete reversal type the stress fluctuates around a mean of zero with a constant amplitude. In repeated type the stress fluctuates around a stress not equal to zero but with a constant amplitude whereas, in random mode both the alternating and mean loads change, either randomly or with a definite pattern.



Complete reversal



Repeated



Random or complicated

Fig. 2.8: Schematics showing types of stress cycling / loading [2.2]

Nucleation and growth of a fatigue crack and the features on the fracture surface are all strongly affected by the shape of the part, the type and magnitude of loading exerted on the part in service, residual stresses, and metallurgical and environmental factors.

2.1.6 Effect of nature of loading on fracture surface appearance

A comprehensive map of macroscopic appearance of possible fatigue failures in laboratory test specimens subjected to a wide range of different loading conditions, stress amplitude with or without stress concentration is offered in Fig 2.9. The two characteristic features are the white area within which less or more curved lines develops, also called as beach marks or arrest lines, and the dark one. The beach marks always depart from a single or more initiation points/origins. Generally, under moderate amplitude loads a single initiation site is observed, while high amplitude loads may generate two or more sites. About the dark area that represents the final overload failure, in general when it is equal or even larger than the clear one containing beach marks, as in the first three columns on the left in Fig.2.9, it means that cyclic loads had high amplitude therefore after a relatively low number of fatigue cycles the remaining section failed by overload. In unidirectional bending the initiation site is located only on one side of the specimen where metal fibers are under tension, while in reverse bending the initiation site may appear on both sides. In rotational bending in which all fibers of the external circumference are equally stressed, the initiation site is randomly located choosing the weakest point exactly as in tension. On the other hand, torsional loading produces a brittle fracture along a helicoidal path or a flat failure if the material behaves in a ductile fashion (not covered in this schematic).

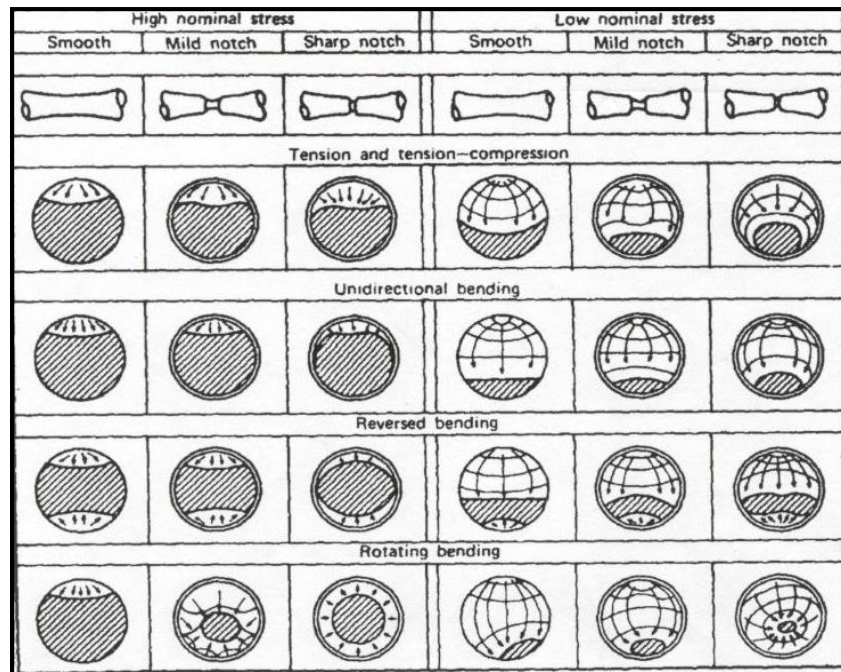


Fig. 2.9: Schematic fracture surfaces for laboratory test specimens subjected to a range of different loading conditions [2.9]

2.1.7 Fatigue evaluation methods

The three major fatigue life estimation methods used in design and analysis are the stress-life method, the strain-life method, and the linear-elastic fracture mechanics method [2.16].

2.1.7.1 Stress-life approach

The safe-life, infinite-life philosophy is the oldest of the approaches to fatigue. The method is based on stress levels only and is the least accurate approach, especially for low-cycle applications. However, it is the most traditional method, since it is the easiest to implement for a wide range of design applications, has ample supporting data, and represents high-cycle applications adequately. This method determines the fatigue strength and/or endurance limit. The results are given in the form of S-N curve i.e. stress versus log number of cycles to failure. Major advantages of this approach are that the load amplitudes are predictable and consistent over the life of the part.

To determine the strength of materials under the action of fatigue loads, specimens are subjected to repeated or varying forces of specified magnitudes while the cycles or stress reversals are counted to point of failure. The most widely used fatigue-testing device is the R. R. Moore high-speed rotating-beam machine. This machine subjects the specimen to pure bending (no transverse shear) by means of

weights. The specimen, is very carefully machined and polished. The results are plotted as an S-N diagram. In the case of ferrous metals and alloys, the curve becomes horizontal (i.e. asymptotic to X-axis) after the material has been stressed for a certain number of cycles. Other types of fatigue-testing machines available apply fluctuating or reversed axial stresses, torsional stresses, or combined stresses to the test specimens

2.1.7.2 Strain-life approach

Strain life is the general approach employed for continuum response in the safe-life, finite-life regime. It is primarily intended to address the low-cycle fatigue area (e.g., from approximately 10^2 to 10^6 cycles). The ϵ - N method can also be used to characterize the “long-life” fatigue behaviour of materials that do not show a fatigue limit. The strain-life method involves more detailed analysis of the plastic deformation at localized regions where the stresses and strains are considered for life estimates. This method gives a reasonably accurate picture of the crack-initiation stage. The results obtained account for cumulative damage due to variations in the cyclic load. Moreover, combinations of fatigue loading and high temperature are better handled by this method. It is applicable for finite-life problems where stresses are high enough to cause local yielding. However, it is the most complicated method to use.

2.1.7.3 Linear elastic fracture mechanics approach

The fracture mechanics method assumes that a crack is already present and detected. It is then employed to predict crack growth with respect to stress intensity. It is most practical when applied to large structures in conjunction with computer codes and a periodic inspection program. This is the best model for studying the crack propagation stage. It is also applied to finite-life problems. It is also used to predict remaining useful life of cracked parts. However, the results rely on the accuracy of the expression for the stress-intensity geometry factor.

2.1.8 Fatigue testing procedure

The determination of fatigue strength of any material is carried out on samples with polished surfaces subjected to repeated or varying loads. Since the fatigue crack initiation is by and large a surface dependent phenomena, proper machining and surface preparation of test samples is of utmost importance. Hence, samples with smooth and uniformly polished surfaces are used. Quite often the fatigue test samples are provided with intentionally machined notches of well-controlled geometry. In either case, the test

samples are cyclically loaded until macroscopically observable cracks initiate and eventually grow to point of failure leading to separation into two pieces. The number of cycles to failure is plotted against the stress amplitude to obtain a fatigue curve.

Based on the fatigue loading mode used during fatigue testing, there are three basic types of fatigue testing machines namely,

- Direct axial loading type machines,
- Plane-bending machines and
- Rotating-beam loading machines

Figure 2.10 (a) and (b) show pictorial views of an axial loading type fatigue testing machine capable of applying both mean and alternating axial loads in tension and/or compression. The principle of operation of such modern servo-hydraulic type axial testing machine includes generating an input signal of load, strain, or displacement using a function generator and applying this input through a hydraulic actuator; measuring the specimen response via a load cell, a clip gage, or a linear variable differential transducer (LVDT); and comparing this with the specific input. Control and test data outputs are usually through a personal computer and commercial or in-house software. The test frequency can range from mHz to kHz. From a small specimen or to components, sub-assemblies, or whole structures can be evaluated for their fatigue behaviour using this kind of machines [2.2].

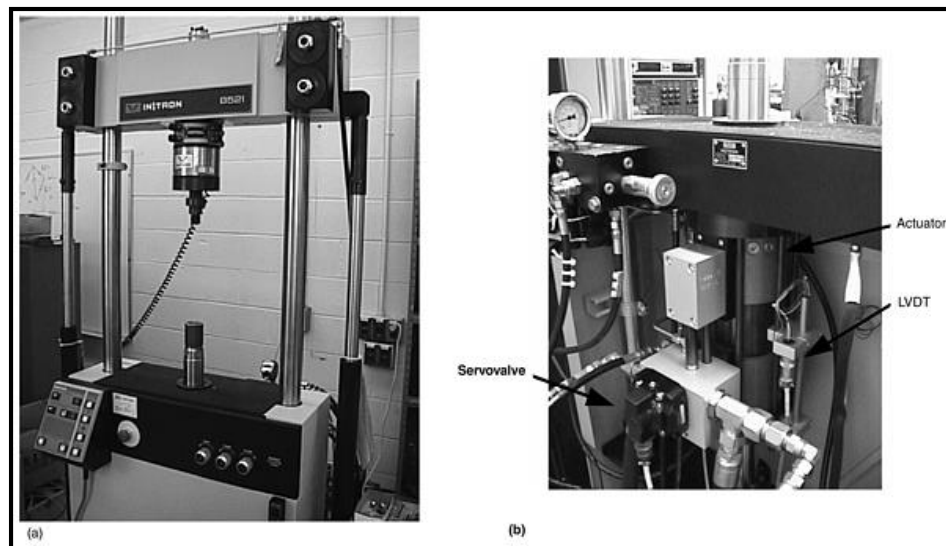


**Fig. 2.10: Modern servo-hydraulic axial fatigue testing machine
(a) Basic load train and (b) Hydraulic actuator, servo valve,
and displacement sensor (LVDT) [2.2]**

Likewise, the schematics of rotating bending machines are shown in Fig. 2.11(a) and (b). Rotating bending machines are generally used to generate a large amount of test

data in a relatively inexpensive way. They are the earliest type of fatigue testing machine, and now a days only occasionally used. Here, the test sample has a round cross section and is subjected to dead-weight loading while swivel bearings permit rotation. Any given point on the circular test-section surface, during each rotation, is subjected to sinusoidal stress variation from tension on the top to compression on the bottom. The four-point bending type test machine shown in Fig. 2.11(b) produces a uniform, pure bending moment over the entire test length of the test sample, while the simple cantilever test machine shown in Fig. 2.11(a) generates a non-uniform bending moment along the length of the sample.

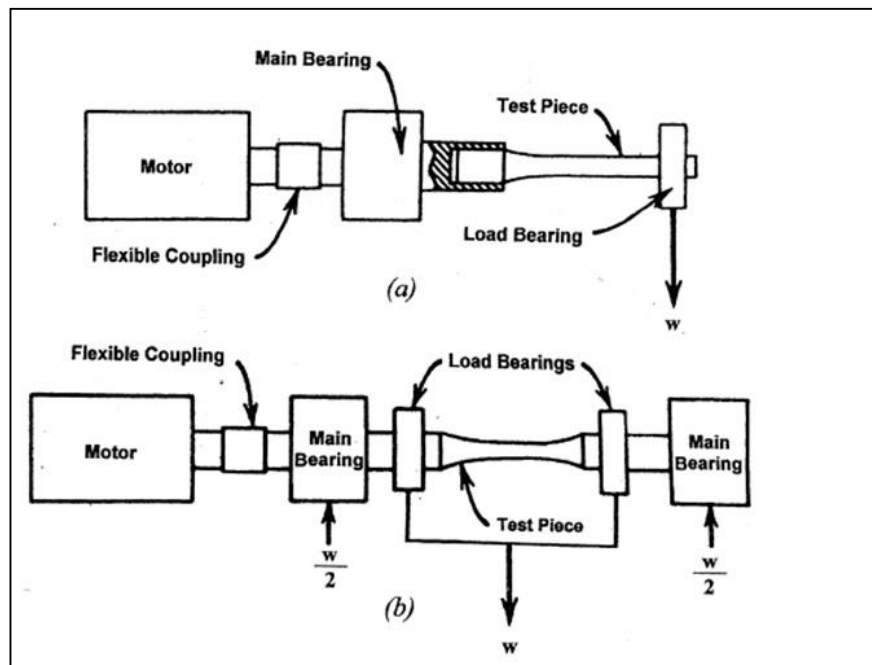


**Fig. 2.11: Schematics of rotating bending fatigue testing machine
(a) Cantilever type and (b) Four point bending type [2.9]**

A pictorial view of a rotating bending type fatigue testing machine is shown in Fig.

2.12 below.



Fig. 2.12: A pictorial view of a rotating bending type fatigue testing machine [Jinan co. China]

The actual sample size and the geometry of the fatigue test sample depend on the type of machine used for fatigue testing. Specimens for direct axial stress machines have a wide range of cross-sectional geometries (solid or hollow) of uniform gage length and round, elliptical, square, rectangular, or thin sheet type axial cross sections [2.9]. Bending fatigue test samples have cross sections of uniform width and thickness for three- or four-point loading, or tapered cross sections for cantilevered plane-bending or rotating-beam testing. Figure 2.13 below gives the schematics of various types of fatigue test samples used with different testing machines.

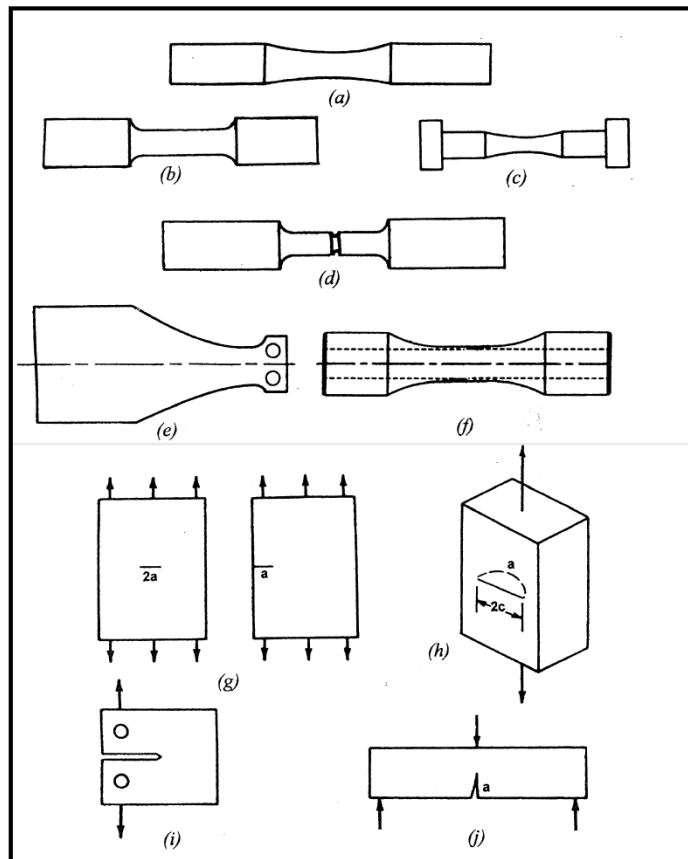


Fig. 2.13: Schematics of various types of fatigue test samples [2.9]

2.1.9 Standard practices related to fatigue testing of metals

Various reference standards are adopted for conducting fatigue testing. These include ASTM, BS, DIN, GOST, ISO, etc. Some of them are listed below.-

ASTM standards:

- E466 Conducting Force Controlled Constant Amplitude Axial Fatigue Tests of Metallic Materials

- E467 Verification of Constant Amplitude Dynamic Forces in an Axial Fatigue Testing System
 - E468 Presentation of Constant Amplitude Fatigue Test Results for Metallic Materials
 - E606 Strain-Controlled Fatigue Testing
 - E647 Measurement of Fatigue Crack Growth Rates
 - E739 Statistical Analysis of Linear or Linearized Stress-Life (S-N) and Strain-Life (s-N) Fatigue Data
 - E1012 Verification of Specimen Alignment under Tensile Loading (under the jurisdiction of Committee E-28 on Mechanical Test Methods)
 - E1049 Cycle Counting in Fatigue Analysis
 - E1823 Standard Terminology Relating to Fatigue and Fracture Testing
- Standard fatigue test methods and procedures for metals are available from ASTM.

2.1.10 Fatigue life diagram or S-N curve

The fatigue tests conducted on samples are normally divided into two types. One type of test focuses on the nominal stress required to cause a fatigue failure in some number of cycles of stress reversals. This type of test is based on Stress-Life approach to fatigue. The basis of the Stress-Life approach to fatigue is the Wohler S-N diagram; also popularly known as S-N Curve, shown schematically for two different materials in Figure 2.14 where applied nominal stress ‘S’ is plotted against total cycles to failure, ‘N’. Most fatigue tests are conducted at “constant amplitude” which means that the maximum and minimum stresses are constant for each cycle of a test. Since the amplitude of the cyclic loading has a major effect on the fatigue performance, the S-N relationship is determined for one specific loading amplitude. The amplitude is expressed as the ‘R ratio value’, which is the minimum peak stress divided by the maximum peak stress. ($R = \sigma_{\min} / \sigma_{\max}$). It is most common to test at an R ratio of 0.1 but families of curves, with each curve at a different R ratio, are often developed.

The data is obtained by cyclically loading smooth or notched specimens until failure. The usual procedure is to test the first specimen at a high peak stress where failure is expected in a fairly short number of cycles. As the stress decreases, the life in terms of number of cycles to failure increases. The test stress is decreased for each succeeding specimen until one or two specimens do not fail in the specified numbers of

cycles, which is usually at least 10^7 cycles. The highest stress at which a run-out (non-failure) occurs is taken as the fatigue threshold or fatigue limit. Not all materials have a fatigue threshold (most nonferrous metallic alloys do not) and for these materials the test is usually terminated after about 10^8 or 5×10^8 cycles. Fatigue limit or *endurance limit* represents a stress level below which the material does not fail and can be cycled infinitely. If the applied stress level is below the endurance limit of the material (represented by the "knee" of the curve), the material is said to have an *infinite life*. The branch point or "knee" of the curve lies normally in the range of 10^5 to 10^7 cycles for materials like low and medium strength steels. In nonferrous alloys there is no stress asymptote and a finite fatigue life exists at any stress level. These materials instead, display a continuously decreasing S-N response. An effective endurance limit for these materials is sometimes defined as the stress that causes failure at 1×10^8 or 5×10^8 loading cycles [2.15 - 2.17].

The S-N Curves are generally reported as semi-log or log-log plot where each point on the curve represents the results of a single test specimen.

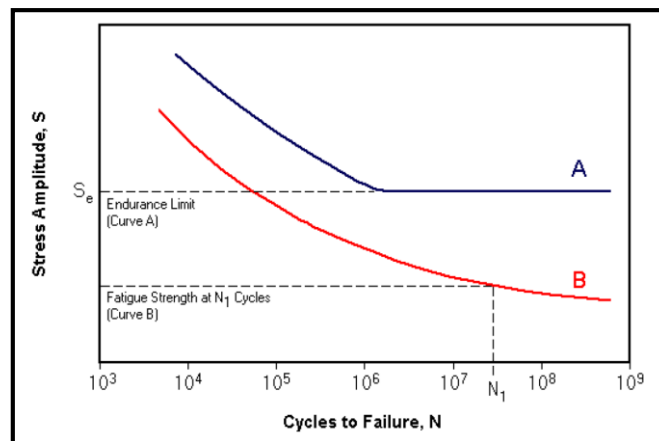


Fig. 2.14: Typical S-N curves for ferrous (curve A, with well defined endurance limit) and Non-ferrous (curve B, without endurance limit) samples [2.17]

When plotted on a log-log scale, a S-N curve can be approximated by a straight line as shown in Figure 2.15.

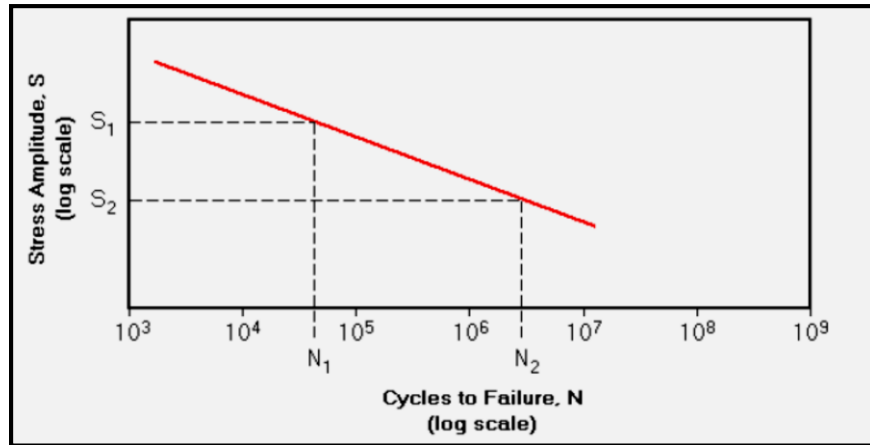


Fig. 2.15: A typical S-N curve on log-log scale, approximated by a straight line. [2.17]

A power law equation can then be used to define the S-N relationship [2.18]:

$$N_1 = N_2 \left(\frac{S_1}{S_2} \right)^{\frac{1}{b}} \quad \text{-----} \quad (2.1)$$

Where b is the slope of the line, referred to as the *Basquin slope*, which is given by:

$$b = \frac{-(\log S_1 - \log S_2)}{\log N_2 - \log N_1} \quad \text{-----} \quad (2.2)$$

Using the value of Basquin slope and any coordinate pair (N, S) on the S-N curve, the power law equation can be used to calculate the cycles to failure for a known stress amplitude.

Another type of fatigue test is the cyclic strain controlled test. In this type of test, the strain amplitude is held constant during cycling. Here, the test sample is subjected to thermal cycling wherein it expands and contracts in response to fluctuations in the operating temperature.

2.1.11 Factors affecting fatigue life

Number of factors govern the fatigue life of a component. They are grouped as mechanical factors and metallurgical factors and discussed in brief here below [2.19]:

Mechanical factors affecting fatigue life

Component size:

Bigger components have larger surface area and since larger surface area has a greater probability of having a flaw, fatigue life sometimes decreases as the component size increases.

Surface condition:

Since in most of the cases the maximum stress is acting at the surface of a component, the fatigue life depends on surface conditions. Tool marks, grinding marks, notches, holes, etc. act as stress raisers and reduce fatigue life. Ground and polished specimens show greater fatigue life than lathe cut rough surface finish. Residual compressive stresses at the surface increase fatigue life whereas the residual tensile stresses decrease it.

Effect of mean stress and stress concentration:

Mean stress also influences fatigue life. Positive tensile mean stress reduces fatigue life whereas negative mean stress may increase it. Mechanical stress raisers such as the fillets or keyways and metallurgical stress raisers like porosity or inclusions reduce the fatigue life.

Metallurgical factors affecting fatigue life

Microstructure:

The fatigue life of components having coarse, angular microstructure is lower than that with a fine, rounded microstructure. For example, at a constant strength level, the fatigue life of a steel having coarse pearlitic structure is lower than that with a spheroidal microstructure because of different morphology of the carbide phase. Same way, the bainitic structure offers greater life than the pearlitic structure.

To a certain extent, the metal with coarse grains have low yield strength and reduced fatigue limit and vice-versa.

Manufacturing process:

Fatigue properties are better in the direction of forging, extrusion and rolling and are lower in the transverse direction. Some processes like shot peening, cold rolling etc. and surface hardening treatments like carburizing, induction hardening or nitriding that induce compressive residual stresses at the surface, reduce the chances of crack initiation and enhance the fatigue properties. Tensile residual stresses on the other hand promote crack initiation.

2.2 Surface engineering

2.2.1 Introduction to surface engineering

Surface engineering refers to a wide range of technologies designed to modify the surface properties of metallic and non-metallic components for functional and/or decorative purposes. One of the objectives of surface engineering is to alter the properties of surface in order to reduce the degradation of the material over a period of time [2.20].

surface engineering or surface modification treatments are used in industry for a variety of reasons including protection against corrosion and wear, rectification of a poor surface quality obtained by normal production methods, improvement in surface appearance, enhancement in fatigue life of a component, etc. Vast majority of surface engineering techniques / treatments are employed to achieve this goal. Some of these treatments are metal cladding [2.20], shot peening [2.21,2.29], hard chrome plating [2.22], electro & electroless plating [2.23], zinc coating / galvanizing [2.24], porcelain enameling [2.25], thermal spraying [2.26], CVD & PVD [2.27], surface hardening via heat treatments like carburizing, nitriding, induction hardening, flame hardening [2.28], etc.

Failure due to fatigue is a result of initiation of a crack, by and large at the surface of the component, and its subsequent propagation as a consequence of cyclic loading of the component. In case of high strength steels under high stress amplitude level, fatigue life is directly related to surface conditions, as the surface has more favorable conditions for nucleation and crack growth than the core, due to geometrical and mechanical conditions [2.30,2.32]. In other words, in such steels the condition of the surface layer plays a more significant role in deciding their fatigue life. Both mechanical as well as metallurgical variables influence the fatigue life. The residual tensile stresses at the surface of a component facilitate the initiation and the propagation of crack at the surface ultimately resulting in failure of the component due to fatigue. Hence, improvement in fatigue resistance in such components can be ensured primarily by decreasing the surface cyclic tensile stress or by increasing the surface yield stress that help in increasing the resistance to fatigue crack nucleation. In practice this can be ensured by changing the characteristics of the surface region of a component by changing its chemical composition and/or its surface microstructure using chemical conversion coatings and/or thermo-mechanical processes. Such modifications develop

residual compressive stresses at the surface of a component leading to enhancement in its fatigue life.

The significance of surface modification treatment with respect to fatigue is associated with three things namely, (i) surface roughness, (ii) residual stresses in the surface layer and (iii) fatigue resistance of the surface layer of the material. All of them can be modified by surface hardening treatment. There are two approaches to surface hardening. One approach does not change composition of the base material and consists of hardening the surface by flame, induction, laser, or electron beam heating. The other approach changes surface composition and include such diffusion techniques as carburizing, nitriding, and carbonitriding.

Some of the industrially used surface hardening methods for introducing residual compressive stresses at the surface of a component to improve the fatigue resistance are: shot peening, cold forming, thermal treatments like case carburizing, nitriding, plasma nitriding, carbonitriding, flame or induction hardening [2.29-2.35], etc.

2.2.2 Various methods of surface treatment

2.2.2.1 Hard chrome plating

Hard chrome plating is a commonly used surface treatment for steel substrates basically because of its excellent surface finish, high corrosion resistance and excellent abrasion & wear resistance. The success of electrolytic hard chrome (EHC) plating relies on the fact that it is cheap and simple; coatings can be obtained in a wide range of thickness, possess an excellent bond strength [2.36-2.37].

Typical process parameters for the conventional hard chromium electroplating consist of a chromic acid solution with 250 g/l of CrO_3 and 2.5 g/l of H_2SO_4 , at 50-55 °C, with a current density ranging from 31 to 46 A/dm², and speed of deposition equal to 25 µm/h using a bath with a single catalyst based on sulphate [2.37].

Despite of several advantages, an important drawback of chromium electroplating is the high tensile residual stresses, originating from the decomposition of chromium hydrides during the electro-deposition process [2.38-2.41]. The high tensile residual stresses developed in electroplated chromium coatings are relieved by formation of local microcracks during electroplating (Fig. 2.16). As the coating thickness increases, tensile stresses increase until the generation of microcracks that relieve them [2.42] The width, depth and population density of these microcracks varies

widely and is influenced by the factors like the type of plating chemistry used (single-catalyst, mixed catalyst, proprietary), chromic acid concentration, type and concentration of catalyst, chromium-to-catalyst ratio, plating current-density, bath temperature, concentration of bath impurities (iron, copper, zinc, nickel, trivalent chromium), etc.

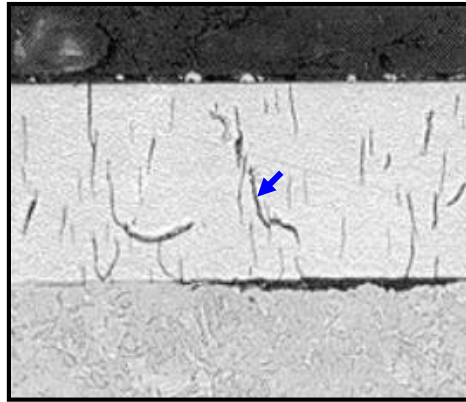


Fig. 2.16: Microcracks in electroplated chromium coating [2.47]

Chromium electroplated AISI 4340 steel features good wear and corrosion resistance due to chromium coating and it is widely used in aeronautical components. But microcracks in chromium layer deriving from the process are prejudicial to component fatigue strength as these cracks rapidly propagate when under cyclic loads as shown in Fig 2.17.

One way to recover fatigue strength of chromium electroplated AISI 4340 steel is to treat its surface with shot peening, inducing compressive residual stresses on surface layers that act as a barrier to microcracks propagation deriving from the chromium coating.

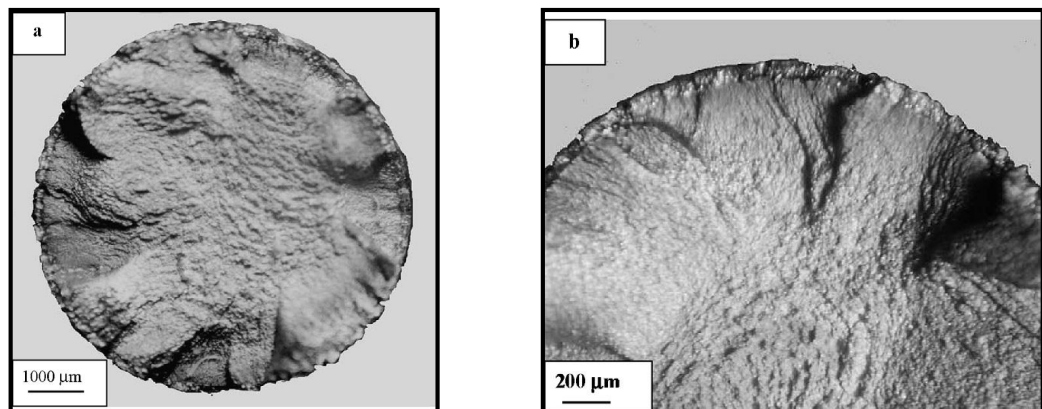


Fig. 2.17: Fracture surface of a hard chrome plated steel showing:
(a) Multiple fatigue cracks initiated at the specimen periphery and
(b) Cracks originating from the coating and extending into the substrate [2.42].

If the attention is focused on fatigue, one of the most widely used surface treatment to enhance the strength of components under cyclic load is shot peening. It consists in “bombing” a surface with a shot flow with energy able to cause plastic deformation of a thin layer of material under the surface. The result is the introduction of a compressive residual stress field near the surface and hardening of the same layer of materials [2.43]. M.A.S. Torres and H.J.C. Voorwald employed shot peening technique to increase the fatigue life of AISI 4340 steel, used in landing gear [2.44]. Shot peening makes the nucleation and propagation of fatigue cracks more difficult [2.37, 2.45]. Rotating bending fatigue tests were conducted by Norihiko HASEGAWA [2.46] over the temperature range from 20 °C to 450 °C were performed on 0.50% carbon steel in annealed and shot peened conditions. It was concluded that shot peening leads to an increase in 26% of fatigue strength compared to annealed conditions at room temperature due to work hardening and compressive residual stress at surface layer.

Realizing the importance of shot peening in improving the fatigue life of various components, Nascimento and co-workers have developed a method to recover the fatigue strength of chromium- electroplated steel by subjecting its surface with shot peening, inducing compressive residual stresses on surface layers that act as a barrier to microcracks propagation deriving from the chromium coating. Accordingly, a shot peening treatment was applied with steel shots in 0.0063 and 0.0083A peening intensities before hard chrome coating. Figures 2.18 shows the fatigue curves for AISI 4340 steel with and without hard chromium plating and with & without shot peening prior to coating. It is apparent from this study that the usage of the shot peening process as a pre-treatment to hard chromium coating is able to recover completely the loss of fatigue strength caused by such coating.

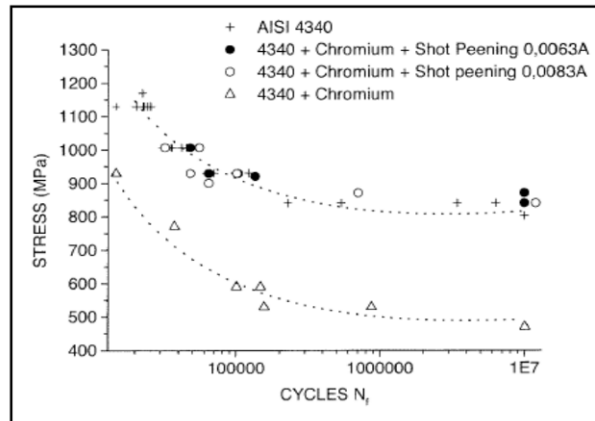


Fig. 2.18: Effect of shot peening pre-treatment on the fatigue behaviour of hard chromium coated AISI 4340 Steel. Shot peening process as a pre-treatment to hard chromium coating is able to recover completely the loss of fatigue strength caused by such coating. [2.49]

Several other workers have also utilized this approach to improve the fatigue strength of steels [2.48-2.51].

2.2.2.2 Induction hardening

Induction hardening is a widely used process for the surface hardening of steel which utilizes the principle of electromagnetic induction to produce heat inside the surface layer of a part. The part to be induction hardened is heated by means of an alternating magnetic field to a temperature within or above the transformation range (i.e. austenitizing temperature) followed by immediate quenching. The core of the component remains unaffected by the treatment whereas only the case gets hardened. The depth of hardening produced by induction heating depends on the factors like frequency of the alternating current, power input, time, part coupling and quench delay [2.52] the treatment does not change the chemical composition of the steel; but merely changes the metallurgical structure to either martensite, bainite or a combination of the two. The plain carbon and alloy steels with an equivalent carbon content in the range 0.40 to 0.45% are most suitable for this process [2.53]. The martensitic or bainitic structure at the surface of the induction hardened part imparts high compressive residual stresses at the surface which improves its resistance to fatigue.

Gregory A. Fett has examined the importance of induction hardened case depth in torsional applications [2.54]. Induction hardened shafts lend themselves very well to most torsional applications because induction hardening increases the hardness near the surface where it is most needed and it leaves the surface in compression, which improves fatigue life. When a shaft is loaded torsionally, the shear stress is highest at the surface and zero at the center. Thus, only the surface needs to be hardened to a depth

to adequately exceed the applied stress. When the surface layer is hardened, martensitic transformation causes it to expand leaving the surface in compression, as opposed to through hardening where the core also expands leaving the surface in tension.

Ground vehicle components such as springs, shafts, and gears are routinely subjected to surface processing treatments to improve mechanical durability. The influence of processes such as shot peening, induction hardening, and carburizing on fatigue performance depends, in a rather complex way, on local material properties, the service loading and, in particular, the magnitude, distribution, and stability of residual stresses. Furthermore, because of the continuing pressures to develop more efficient and lighter weight structures, there is considerable interest in maximizing the benefits of surface processing.

Gerber, T. L. and Fuchs, H. O. have studied the residual stress effects on fatigue of surface processed steels [2.55-2.57]. The study reveals that for induction hardening, the residual stress pattern depends upon the depth of hardening and, in general, relates to the hardness profile.

2.2.2.3 Thermal spray methods

Thermal spray is a generic term for a group of processes [2.58-2.60] in which metallic, ceramic, cermet, and some polymeric materials in the form of powder, wire, or rod are fed to a torch or gun with which they are heated to near or somewhat above their melting point. The resulting molten or nearly molten droplets of material are accelerated in a gas stream and projected against the surface to be coated (i.e. the substrate). On impact, the droplets flow into thin lamellar particles adhering to the surface, overlapping and interlocking as they solidify. The total coating thickness is usually generated in multiple passes of the coating device. The basic principle of thermal spray processes is given in following schematic.

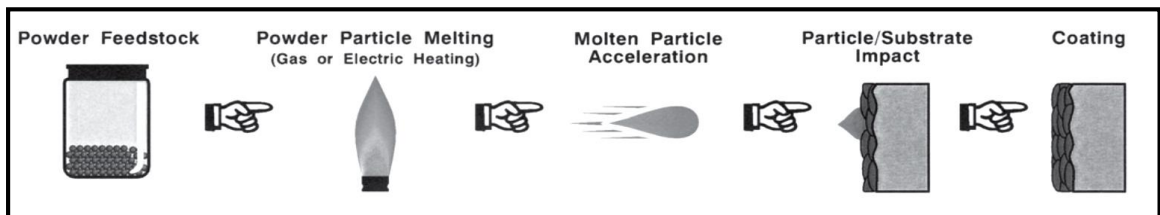


Fig. 2.19: Schematic of thermal spray process [2.61]

Some the advantages of the thermal spray processes include (i) ability to cover the extremely wide variety of materials that can be used to make a coatings, virtually any material that melts without decomposing can be used (ii) ability of most of the thermal spray processes to apply a coating to a substrate without significantly heating it. Thus, materials with very high melting points can be applied to finally machined, fully heat-treated parts without changing the properties of the part and without thermal distortion of the part and (iii) the ability to strip and recoat worn or damaged coatings without changing the properties or dimensions of the part. However, a major disadvantage of thermal spray processes is that they are 'line-of-sight' type processes i.e. they can coat only those areas that the torch or gun can "see."

The applications of thermal spray coatings are extremely varied. To name a few are: to enhance the wear and/or corrosion resistance of a surface, for dimensional restoration, as thermal barriers, as thermal conductors, as electrical conductors or resistors, for electromagnetic shielding, and to enhance or retard radiation, to enhance the fatigue life of a material. Thermal spray processes are hence used in virtually every industry, including aerospace, agricultural implements, automotive, primary metals, mining, paper, oil and gas production, chemicals and plastics, and biomedical.

There are three basic groups of thermal spray processes based on the method of energy generation viz. processes based on energy generation (i) by compressed gas expansion known as cold spray process, (ii) by combustion spraying using combustion spray guns like Flame Spray gun, High Velocity Oxy-fuel Flame (HVOF) and Detonation gun or D-gun and (iii) by electrical discharge plasma spraying involving the use of direct current (D.C.) plasma torches, direct current (D.C.) transferred arc plasma and wire-arc spraying approach.

Different thermal spray processes can also be classified as follows on the basis of heat source used.

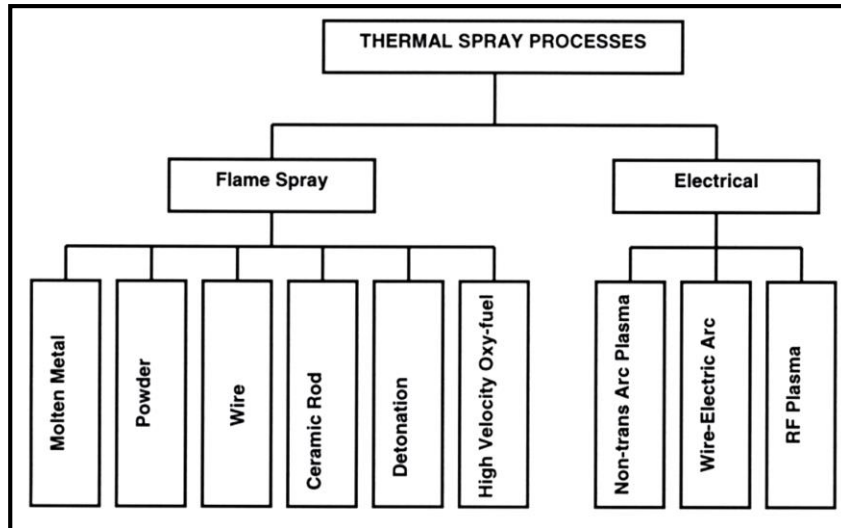


Fig. 2.20: Classification of thermal spray processes on the basis of heat source [2.61]

Of all these processes the Flame Spray process, High Velocity Oxy-Fuel (HVOF) process and Detonating-gun process are discussed further, being industrially more important and frequently used techniques.

2.2.2.3.1 Flame spray processes

Flame spray, also known as oxy/acetylene combustion spray is the original thermal spray technique developed about 100 years ago. Dr. Max Ulrick Schoop of Zurich recognized the possibility that a stream of molten particles impinging upon themselves could create a coating. His work, and that of his collaborators, resulted in the establishment of the thermal spray process. The flame spray process is characterized by low capital investment, high deposition rates and efficiencies, and relative ease of operation and low cost of equipment maintenance.

Flame spray process works on the basic principles of a welding torch with the addition of a high velocity air stream to propel molten particles onto the substrate. It uses combustible gas as a heat source to melt the coating material usually in the form of a wire. Acetylene, propane, methyl-acetylene-propadiene (MAPP) gas, and hydrogen, along with oxygen, are commonly used flame spray gases. Flame spray guns are available to spray materials in rod, wire, or powder form.

Flame Powder Spray process uses a similar technique as the Flame Wire Spray process, except that the wire feedstock is replaced with a powder. The main advantage of this process is that a much wider range of materials (including nickel or cobalt- base superalloys or ceramic materials) can be easily processed into powder form giving a

larger choice of coatings. Not only this, the alloys which are difficult or cannot be produced in a wire form can also be processed as coating by this route. In this process, a chemical reaction between oxygen and a fuel of combustion acts as a heat source. This heat source creates a gas stream with a temperature in excess of 3,000 °C with correctly balanced conditions between oxygen and acetylene. Flame velocities below 100 m/s characterize this process. The feed stock material to be sprayed is fed into the flame in the form of a powder to melt and the thermal expansion of the combustion is then used to atomize and accelerate the particles onto the substrate forming a coating. The pictorial view of Flame Powder Spray process is given in Fig. 2.21.

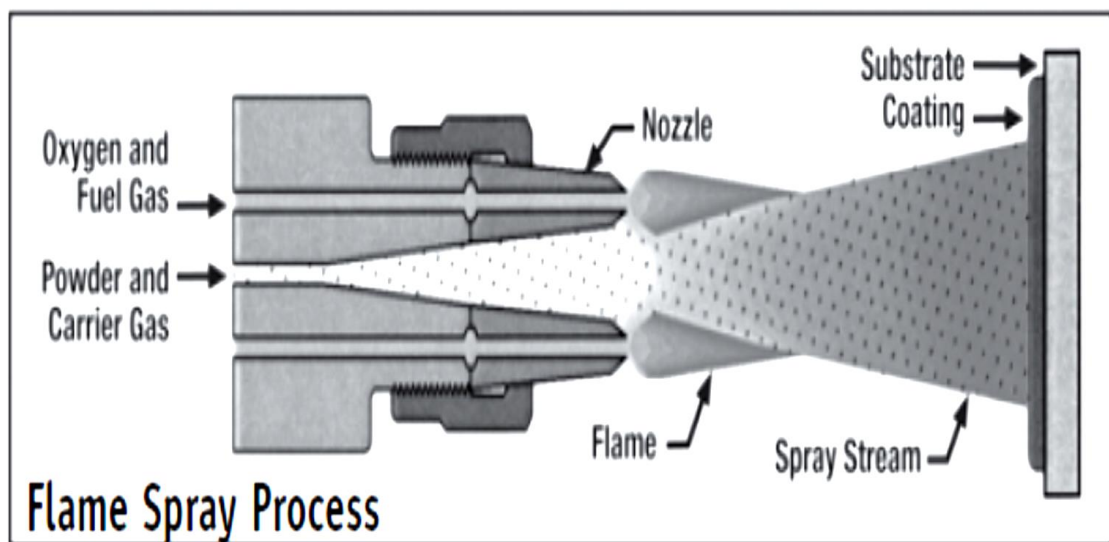


Fig. 2.21: Schematic view of flame powder spray process [2.61]

2.2.2.3.2 High velocity Oxy-Fuel (HVOF) process:

High Velocity Oxy-fuel (HVOF) is the coating process most often used for hard chrome coating replacement. Tungsten-carbide Cobalt-Chrome (WC-CoCr) and Chromium-carbide Nickel-Chrome (CrC-NiCr) are two of the most common powder materials used to replace hard chrome coating. HVOF was invented in the early 1980's. During this time Browning and Witfield, using rocket engine technologies, introduced a unique method of spraying metal powders. The technique was referred to as High Velocity Oxy-Fuel (HVOF). The process utilizes a combination of oxygen with various fuel gases including hydrogen, propane, propylene, hydrogen and even kerosene. Powders to be sprayed via HVOF are injected axially into the expanding hot gases where they are propelled forward, heated and accelerated onto a surface to form a

coating. Gas velocities exceeding Mach 1 and powder velocity of the order of 550 m/s have been reported with temperatures approaching 2,300 °C. Modern HVOF guns offer powder particle velocities of the order of 850 m/s. Coating thicknesses are usually in the range of 0.05 to 0.50 mm, but substantially thicker coatings can also be produced. Not only this, the high impact velocity of sprayed particles in HVOF process helps in generating residual compressive stresses on the surface of a component responsible for improvement in its fatigue life.

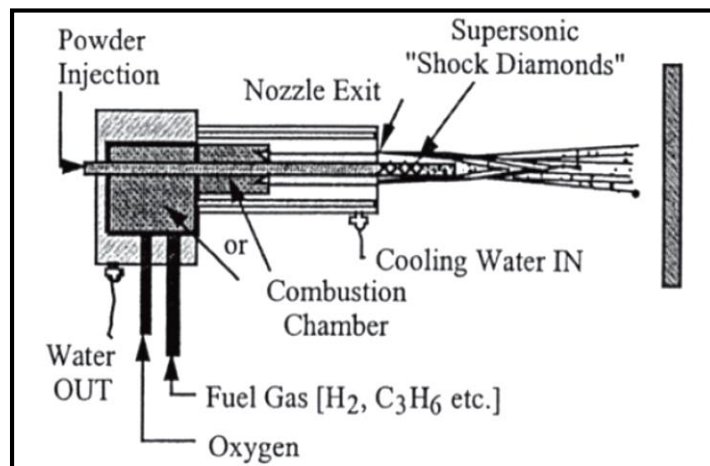


Fig. 2.22: Schematic view of HVOF process [2.61]

2.2.2.3.3 Detonation gun spray process:

This process is a variation of “thermal spray process” in which the controlled explosion of a mixture of fuel gas, oxygen, and powdered coating material is utilized to melt and propel the material to the work piece. First developed in Russia it was introduced in the early 1950s by Gfeller and Baiker working for Union Carbide.

The detonation by a spark is generated using acetylene or hydrogen–oxygen mixtures (with some nitrogen to modify the detonation parameters) contained in a tube closed at one end. The high-temperature, high-pressure detonation wave moving down the barrel heats the powder particles to their melting points or above and accelerates them to the substrate at high velocity. Gas velocities of more than 2,000 m/s are achieved. Contrary to the two previous devices where combustible gases and powders are continuously fed into the gun, combustible gases and the powders are fed in the D-gun in cycles repeated at a frequency of 3–100 Hz. Detonation gun coatings have some of the highest bond strengths and lowest porosities of the thermal spray coatings. In

fact, they have been the bench-mark against which the other coatings have been measured for years.

The prime advantages of this process are higher density, improved corrosion barrier, higher hardness; better wear resistance, higher bonding and cohesive strength, almost no oxidation, thicker coatings, and smoother as-sprayed surfaces.

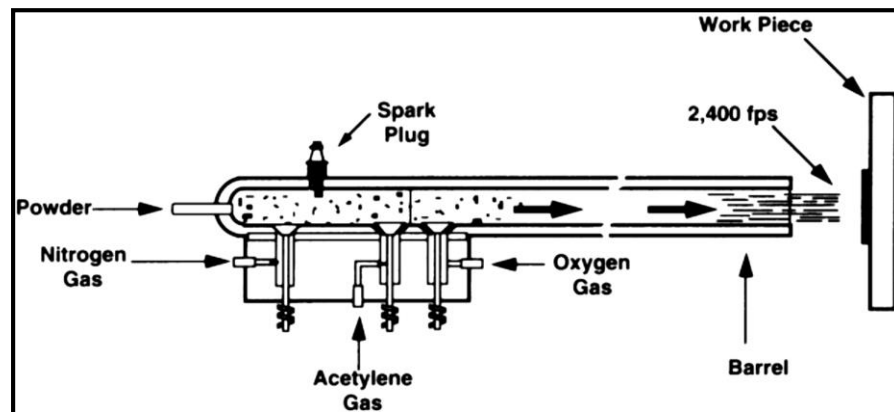


Fig. 2.23: Detonation gun spray process [2.61]

2.2.2.3.4 Electric wire-arc process

Electric wire-arc thermal spraying utilizes the same principles employed in wire arc welding systems. This process differs from other thermal spray processes in that there are no external heat sources as in any the combustion gas/flame spray processes. Instead, the coating material, in wire form, is electrically charged and then contacted creating an arc. The molten droplets of metal formed on tip of the wire are then sprayed onto the substrate using a high velocity air stream to atomize and propel the material. Electric arc spraying process has the advantage of not requiring the use of oxygen and/or a combustible gas; has the ability to process metals at high spray rates; and is, in many cases, less expensive to operate than either plasma and/or wire flame spraying [2.61].

Of all the thermal spray processes discussed above, the HVOF process has drawn the maximum attention.

As discussed earlier, High Velocity Oxy-fuel (HVOF) spray technique is one of the leading technologies that have been proposed as a feasible alternative to the replacement of electrolytic hard chromium (EHC) plating in a number of engineering applications. In the past few years, significant efforts have been made to substitute EHC

due mainly to the numerous environmental hazards involved in its production. Chromium plating baths contain chromic acid solutions, in which the chromium is in the hexavalent state, with hexavalent chromium (hex-Cr) and several catalytic anions being known as carcinogenic substances. HVOF constitutes a more friendly deposition process from the environmental point of view, which has already been employed successfully for the replacement of EHC by means of other ceramic coatings [2.62-2.65]. Such coatings are characterized by possessing a high density and good adherence to the substrate.

R.C. Souza, H.J.C. Voorwald and M.O.H. Cioffi compared the influence of $\text{Cr}_3\text{C}_2\text{-25NiCr}$ and WC-10Ni coatings applied by HVOF process and hard chromium electroplating on the fatigue strength, abrasive wear and corrosion resistance of AISI 4340 steel [2.66]. The S–N curves were obtained in axial fatigue tests for base material, chromium plated and HVOF coated specimens. The effect of chromium electroplating was to decrease the axial fatigue strength of AISI 4340 steel. As against this, the thermally sprayed $\text{Cr}_3\text{C}_2\text{-25NiCr}$ results in higher fatigue strength when compared to chromium electroplated. In comparison to bare AISI 4340 steel, reduction in fatigue life, for high cycle fatigue, occurred. With respect to WC-10Ni thermal spray coated specimens, insignificant influence on the fatigue strength was detected.

Fatigue behaviour of different low-alloy steels such as SAE 1045 steel, AISI 4140 steel, AISI 4340 steel, etc. in uncoated and coated condition with different HVOF coatings like Colmonoy 88 alloy (NiCrBSiW) and cermets like WC-Co , WC-10Co-4Cr , Co-Mo-Cr , etc. has been studied by several researchers [2.67-2.73]. Prior to deposition the samples are generally grit-blasted with alumina particles for better adhesion of the coating with the steel substrate. However, the analysis of the fatigue fracture surfaces of the samples tested in air reveal that alumina particles present on the surface of the grit-blasted samples remain embedded at the surface of the material, act as stress concentrators, inducing the nucleation of fatigue cracks at the substrate-coating interface, resulting in the reduction in fatigue life (Fig. 2.24). However, under corrosive conditions and low alternating stresses, the presence of the coating provides an effective protection against corrosion-fatigue failures, giving rise to an improvement of the corrosion-fatigue performance of the coated system.

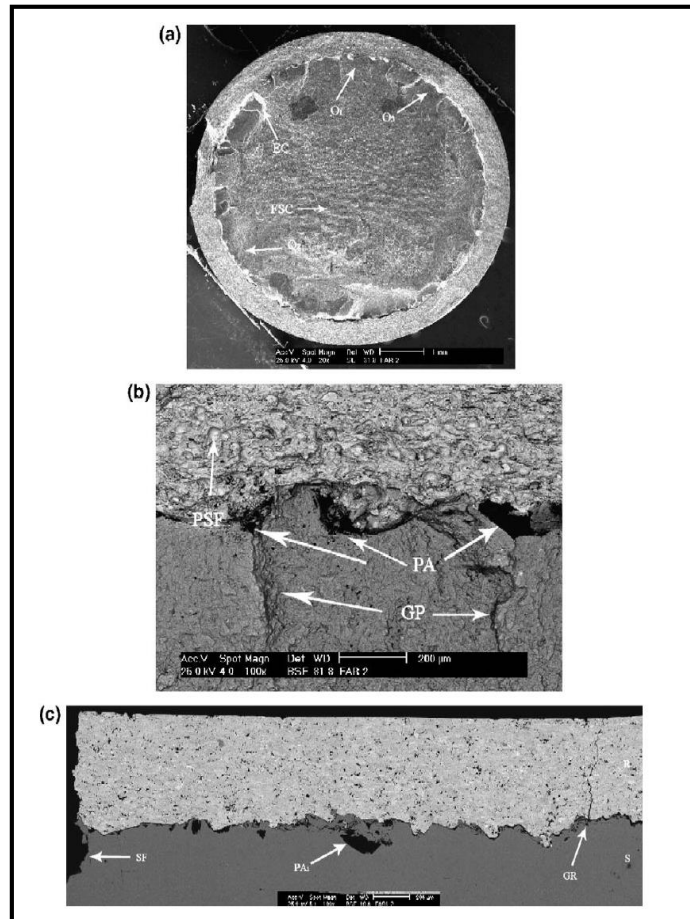


Fig. 2. 24: Fracture surface of a coated sample showing
(a) Nucleation and growth of multiple fatigue cracks
(b) Crack initiation site showing the presence of alumina particles (PA)
from which fatigue cracks grow
(c) Cross-sectional view illustrating the presence of alumina particles
(PA1) and cracks (GR) within the coating [Ref 2.67]

Thus the results of the above investigations indicate that grit blasting the base steel could lead to a significant reduction in the fatigue properties of the material.

E.S. Puchi Cabrera and K. Padila [2.74, 2.76] investigated the fatigue properties of an AISI 4140 steel in a quenched and tempered (Q&T) condition, coated with a deposit of Colmonoy 88 alloy, applied by HVOF thermal spray. An intermediate-bonding layer of Metco 447 (a proprietary alloy), also applied by HVOF thermal spraying was used to avoid grit blasting the steel substrate with alumina particles. The study was mainly conducted in order to assess, if the elimination of the grit blasting step could give rise to an improvement in the fatigue performance of the coated material, given the absence of alumina particles retained in the steel substrate, which in previous studies were identified as stress concentrators responsible for the nucleation

of fatigue cracks. It was found that coating the steel substrate with such a deposit lead to a significant reduction in fatigue properties in comparison with the uncoated substrate.

Shot peening has also been tried out as one of the surface preparation approach prior to HVOF coating. The influence of shot peening treatment on the axial fatigue strength of WC-10Ni HVOF thermal spray coated AISI 4340 steel, was evaluated [2.77]. In order to study the influence of residual stresses on fatigue life, the stress field was measured by X-ray tensometry. Scanning electron microscopy was used to investigate the fatigue source appearance. For WC-10Ni thermal- spray coated shot-peened material the fatigue strength was restored, reaching results close to base material. The HVOF thermal spray process reduced the tensile residual stresses on base metal specimen surface. The shot peening process increased the axial fatigue strength of AISI 4340 steel WC-10Ni thermal spray coated specimens by 13.3% from 750 MPa to 850 MPa.

The aim of the study conducted by M.P. Nascimento and co-workers [2.78] was to analyse the effects of tungsten carbide thermal spray coating applied by HP/HVOF process; chemical nickel underplate, and shot peening process applied before coating deposition on AISI 4340 steel in its rotating bending fatigue behaviour, in comparison to hard chromium electroplating. Rotating bending fatigue test results indicated better performance for the conventional hard chromium plating in relation to the accelerated hard chromium electroplating. Tungsten carbide thermal spray coating and accelerated hard chromium plate over nickel resulted in higher fatigue strength when compared to samples that were conventional or accelerated hard chromium plated. Shot peening proved to be an excellent alternative to increase fatigue strength of AISI 4340 steel hard chromium electroplated.

Similarly, Tipton [2.79] conducted an investigation, in order to examine the effect of some HVOF thermally sprayed coatings including, WC-17% Co, Cr₃C₂-20% NiCr and Inconel 625, with thickness in the range of 200–400 μm, on the room and elevated temperature high-cycle fatigue behaviour of an AISI 403 (martensitic) stainless steel, tested under rotating bending conditions at room temperature, 477 and 700 K. According to this author, in some cases an increase in fatigue properties was observed, whereas, in others a reduction in such properties could also be noticed.

An investigation has been carried out by [2.80] in order to study the fatigue performance, both in air and in a 3 wt.% NaCl solution, of a quenched and tempered

(Q&T) SAE 4340 steel substrate coated with a TiCN film of ~ 4 micron in thickness deposited by plasma assisted physical vapor deposition (PAPVD). The present investigation has shown that coating a Q&T 4340 steel substrate with a TiCN film of ~4 micron in thickness deposited by PAPVD can provide a significant increase, in the range of ~140–180%, in fatigue life, in comparison with the uncoated substrate, when the material is tested in air under rotating bending conditions at maximum alternating stresses in the range of ~550–700 MPa. However, when the material is tested in a 3 wt.% NaCl solution only a marginal increase (25% at the most) in the number of cycles to failure is observed.

There are reports on the rolling contact fatigue (RCF) behaviour of HVOF coated steels as well. Attempts have been made to investigate the contact fatigue behaviour of steels in terms of the influence of coating thickness and contact stress fields on the performance and fatigue failure modes of thermal spray (WC–12%Co) HVOF coatings [2.81]. Results of this study indicate that a non-dimensional coating thickness parameter ($\Delta = \xi/\Psi$), where ξ is the coating thickness and Ψ the depth of maximum shear stress, can be used as a useful index to optimise coating delamination resistance during Hertzian contact loading. The rolling contact fatigue (RCF) investigations of the HVOF coatings on 440-C steel indicated that by appropriate control of coating thickness ($\Delta \geq 1.5$), and tribological conditions of contact stresses and lubrication, it is possible to achieve a fatigue life in excess of 70 million stress cycles without failure.

The rolling contact fatigue (RCF) behaviour of thermally sprayed WC-Co coatings with nominal compositions of WC-12%Co, WC-10%Co-4%Cr and WC-17%Co was studied with a two-roll configuration roll-against-roll testing apparatus under 420-600 MPa Hertzian contact stresses in unlubricated pure rolling conditions [2.82]. The coatings were prepared by Atmospheric Plasma Spray (APS) and two High Velocity Oxyfuel (HVOF) spray processes. In the APS sprayed WC-12%Co coating, the RCF damage was dominated by an increased surface roughness due to spallation of flakes and a formation of a network of cracks within the coating layer. HVOF sprayed WC-12%Co and WC-10%Co-4%Cr coatings were damaged either by the formation of vertical, linear cracks or pitting of the contact surface. The formation of pits in the HVOF sprayed coatings was significantly less than that found in the APS sprayed coating. The HVOF sprayed WC-17%Co coating showed the best RCF behaviour among the studied coatings with unchanged surface roughness, no formation of cracks and only a few pits were found on the contact surface. The good resistance of this

coating against formation of failure in the RCF testing is caused by its higher ductility and fracture toughness due to a higher metallic binder content in comparison with the other coatings.

R. Ahmed and M. Hadfield [2.83] have taken a holistic approach to summarize the results of ongoing research on various cermet (WC-Co) and ceramic (Al_2O_3) coatings deposited by detonation gun (D-Gun), high-velocity oxyfuel (HVOF), and high-velocity plasma spraying (HVPS) techniques, in a range of coating thickness (20-250 μm) on various steel substrates to deliver an overview of the various competing failure modes. Results indicate four distinct modes of fatigue failure in thermal spray cermet and ceramic coatings namely abrasion, delamination, bulk failure, and spalling. These failure modes compete during fatigue failure and eventual coating failure may be either due to one or a combination of these modes. The influences of coating process, thickness, materials, properties of substrate materials, and pre-spray conditions on these fatigue failure modes are also examined using scanning electron microscopy (SEM), electron probe microscopy analysis (EPMA), and surface interferometry, as well as subsurface observations using x-ray diffraction (XRD), residual stress analysis, and dye-penetrant investigations. Coating failures were attributed to micro- and macrocracking of either the coating material or the coating substrate interface, which also resulted in the attenuation of compressive residual stress.

2.2.2.4 Nitriding

2.2.2.4.1 Basics of nitriding

One of the ways to obtain complex surface physical and mechanical properties of metallic materials such as hardness, wear resistance, fatigue resistance, corrosion resistance and others is chemical heat treatment method – nitriding [2.84-2.86]. The nitriding process, first developed in the early 1900s, continues to play an important role in the manufacture of aircraft, bearings, automotive components, textile machinery, and turbine generation systems to name a few.

Nitriding is a group of surface-hardening processes based on the thermo-chemical principle involving introduction of nitrogen into the surface of the steel. Nitriding produces a strong and shallow case with high compressive residual stresses on the surface of steel components such as axles, shafts, gears, crankshafts, dies and tools so as to improve their fatigue life. It is a process for hardening the surface of a metal by diffusing nitrogen into the surface. Conventionally this is done in an ammonia

atmosphere or a special nitrogen-containing salt bath. Commercially used various nitriding processes are liquid or salt bath nitriding, gas nitriding, and plasma or ion nitriding.

Salt bath nitriding process is carried out in a molten salt bath. The nitrogen penetrating the surface of a component is derived from a liquid medium consisting of molten salts containing cyanides or cyanates. The temperature of the salt bath is usually between 400 and 600 °C. The cyanate undergoes catalytic decomposition on the steel surfaces at these temperatures to form cyanide, carbonate and adsorbed nitrogen. Being an old technology with a negative impact on the environment, salt bath nitriding process is increasingly being replaced by gas or plasma nitriding in industrial use.

In gas nitriding, nitrogen is introduced into a steel surface from a controlled atmosphere by holding the metal at a suitable temperature in contact with a nitrogenous gas, usually ammonia, NH₃. The catalytic decomposition of ammonia provides the required active nitrogen for diffusion into the surface of a material to be nitrided.

The ion, or plasma nitriding process uses plasma-discharge technology at lower temperature to introduce nascent nitrogen on the steel surface. Plasma is formed by high-voltage electrical energy in vacuum. Nitrogen ions are then accelerated to impinge on the component to be nitrided which is connected as a cathode. The ion bombardment heats the work piece, cleans the surface and provides the nascent nitrogen for diffusion into the steel material. Table 2.1 below gives a comparative idea of the different nitriding processes at a glance.

Table 2.1: Different nitriding processes at a glance

Process	Nature of medium	Process Temp. (° C)	Typical case depth (µm)	Case Hardness (HV)	Typical base metals	Process characteristics
Gas	Ammonia gas	480-590	125-700	550-1200	Alloy steels, Nitriding steels, Stainless steels	Hardest cases from nitriding steels, quenching not required, low distortion, Process is slow, usually a batch process.
Salt	Cyanide based salts	510-565	25-750	550-1200	Most Ferrous metals including Cast irons	Usually used for thin hard cases less than 25 microns, no white layer, rest are proprietary processes
Plasma	Nitrogen-Hydrogen gas mixture	340-565	75-750	550-1200	Alloy steels, Nitriding steels, Stainless steels	Faster than gas nitriding, no white layer, higher, Excellent control on process and case depth, Excellent reproducibility

(Courtesy : Milman Thin Film Systems Pvt. Ltd., Pune; milman@vsnl.com)

Nitrided steels are generally medium-carbon (quenched and tempered) steels that contain strong nitride-forming elements such as aluminum, chromium, vanadium, and molybdenum. The most significant hardening is achieved with a class of alloy steels (nitralloy type) that contain about 1% Al. When these steels are nitrided, the aluminum forms AlN particles, which strain the ferrite lattice and give rise to dislocation strengthening. Titanium and chromium are also used to enhance case hardness, although case depth decreases as alloy content increases. Usually alloy steels in the heat-treated (quenched and tempered) state are used for nitriding [2.87].

Nitriding consists of the inward diffusion of nitrogen into the material; the nitrogen is absorbed through the surface of the material. This diffusion process is based on the solubility of nitrogen in iron, as shown in the iron-nitrogen equilibrium diagram (Fig. 2.25) [2.87].

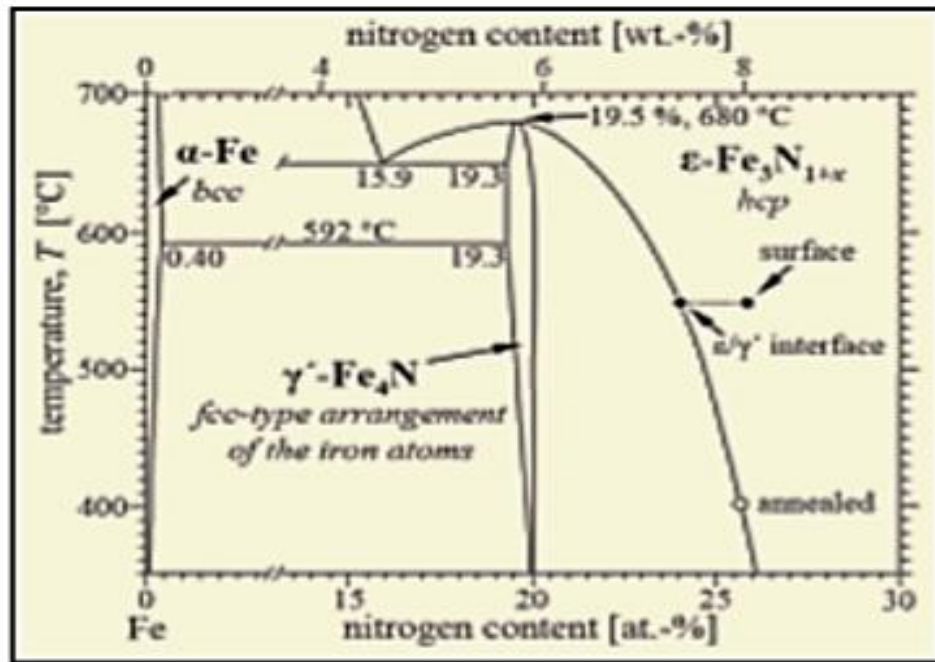


Fig. 2.25: Part of the Iron-nitrogen equilibrium diagram showing formation of Fe₄N intermetallic phase [2.87]

The solubility limit of nitrogen in iron is temperature dependent, and at 450 °C (840 °F) the iron-base alloy will absorb up to 5.7 to 6.1% of N. Beyond this, the surface phase formation on alloy steels tends to be predominantly epsilon (ϵ) phase. This is strongly influenced by the carbon content of the steel; the greater the carbon content, the more potential for the ϵ phase to form. As the temperature is further increased to the gamma prime (γ') phase temperature at 490 °C (914 °F), the “window” or limit of solubility begins to decrease at a temperature of approximately 680 °C (1256 °F). The

equilibrium diagram thus shows that control of the nitrogen diffusion is critical to process success [2.87].

2.2.2.4.2 Structure and composition of nitrided layer:

The secret of the nitriding process is that it does not require a phase change from ferrite to austenite, nor does it require a further change from austenite to martensite unlike other surface hardening processes such as carburizing or induction hardening. In other words, the steel remains as ferrite phase (or cementite, depending on alloy composition) during the complete procedure [2.87]. Nitriding is usually performed at temperature between 500 and 560 °C where the structure of the steel is still ferritic. Nitrogen diffusion modifies surface and near surface microstructure producing hard layers with altered mechanical properties.

The principal phases that form during the nitriding of iron- base materials are: (i) solid solution of alpha-iron (α) (which has a maximum solid solubility of about 0.11 wt.% nitrogen), (ii) the phase gamma-prime (γ') (which has a solubility range of about 5.1 to 6.1 wt.% nitrogen depending on temperature and is usually represented by the chemical formula Fe_4N), and (iii) the epsilon phase (ϵ) (Fe_{2-3}N) (it may have equilibrium nitrogen content of 7 to 8 wt.% nitrogen, depending on the temperature at which it forms).

The phases γ' and ϵ can be conceived as typical interstitial compounds with the iron atoms arranged in a cubic close-packed fashion in the γ' phase and in a hexagonal close-packed fashion in the ϵ phase and have the following crystal structures [2.88].

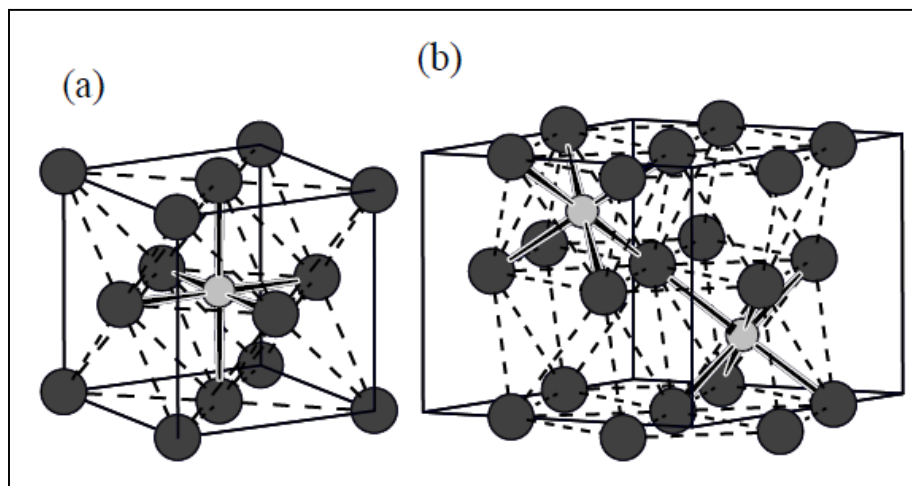


Fig. 2.26: Crystal structure of (a) γ' - $\text{Fe}_4\text{N}_{1-y}$, (b) ϵ - $\text{Fe}_3\text{N}_{1+x}$. (The darker spheres represent the iron atoms and the lighter spheres the nitrogen and carbon atoms) [2.142]

The layer on the nitrided steel consists of two parts, a compound layer which is typically 2 to 20 μm thick, hard and chemically resistant and beneath it a tougher diffusion layer with a thickness of 0.1 to 0.8 mm. The case structure of a nitrided steel, consists of a diffusion layer with or without a compound layer. Figure 2.27 gives the variation in hardness with respect to thickness of the nitrided layer for compound and diffusion layer.

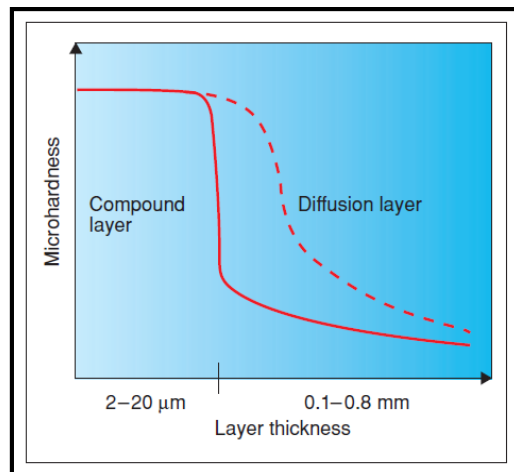


Fig.2.27: Variation in hardness with respect to thickness of the nitrided layer for compound and diffusion layer. Microhardness drastically decreases above a certain value of layer thickness [2.88]

The compound layer assumes one of the three following forms, according to the depth-dependent concentration distributions of nitrogen:

- a γ' -compound layer (γ' -nitride: Fe_4N)
- an ϵ -compound layer containing more nitrogen (ϵ -nitride: Fe_{2-3}N)
- a mixed-phase compound layer (γ' -nitride Fe_4N and ϵ -nitride Fe_{2-3}N).

The compound layer [2.89] is also known as 'white layer' because of its white color after Nital etch on the microscopy and has a thickness of some micrometers. The compound layer quite is often made up of the region where the γ' (Fe_4N) and ϵ (Fe_{2-3}N) intermetallics are formed. Thickness and phase content of compound layer depend on the treatment parameters such as specific gas composition, time and temperature of nitriding, etc. [2.90, 2.91]. Because the 'white layer or compound layer' is hard and brittle its formation is usually avoided or at least kept small. The layer, beneath the compound layer, is known as 'diffusion layer' which consists of mainly interstitial atoms in solid solution and fine coherent nitride precipitates when the solubility limit is reached. In other words the diffusion layer of a nitrided case can best be described as

the original core microstructure with some solid solution and precipitation strengthening. It is in the subsurface of a steel component with a gradual reduction in the hardness and nitrogen concentration towards the core, resulting in a diffuse case-core interface. The thickness of the diffusion layer is also known as ‘case depth’. The depth of the diffusion layer depends on the nitrogen concentration gradient, time at a given temperature, and the chemistry of the workpiece. As the nitrogen concentration increases toward the surface, very fine, coherent precipitates are formed when the solubility limit of nitrogen is exceeded. The precipitates can exist both in the grain boundaries and within the lattice structure of the grains themselves. These precipitates, nitrides of iron or other metals, distort the lattice and pin crystal dislocations and thereby substantially increase the hardness of the material. Though the diffusion layer is relatively thick and strong, in most ferrous alloys, the diffusion layer formed by nitriding cannot be seen in a metallograph because the coherent precipitates are generally not large enough to resolve. Characteristics of compound layer are high hardness (800 to 1400 Hv), greatly improved wear and corrosion resistance, reduced adhesion, reduced tribo-oxidation; while diffusion layer provides hardness gradient to the base material and is responsible for a considerable enhancement of the fatigue endurance against flexural and torsional stress. The fatigue properties are principally determined by the macro- and microstress state within the diffusion zone. Figure 2.28 gives the schematics of nitrided case structure whereas Fig. 2.29 shows the optical micrograph of layers formed in a nitrided sample.

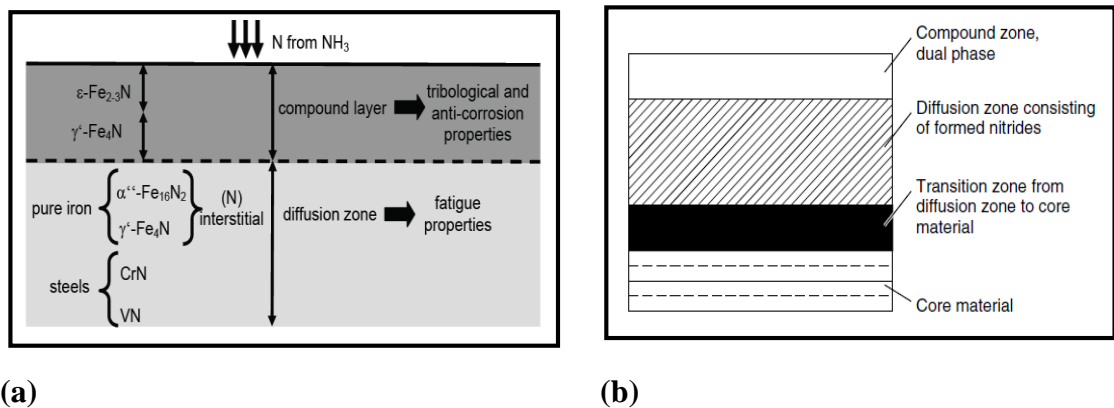


Fig.2.28: Schematics of the nitrided case structure on iron/iron-base alloys showing different phases developed [2.92]

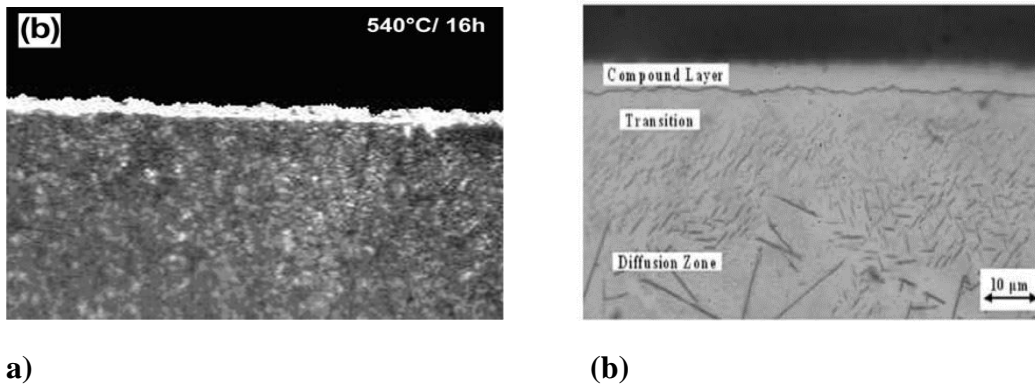


Fig. 2.29 : Typical optical micrographs showing the layers formed in a nitrated sample [2.93, 2.94]

The effect of nitriding on fatigue life has been extensively studied by several researchers for a variety of steels including AISI 1045 steel [2.95], Cr-Ni-Mo steel [2.96], AISI 4340 steel [2.100], AISI 4140 steel [2.98, 2.99, 2.104], Cr-Mo steel [2.101] & Cr-Mo-V steel [2.97, 2.104-2.106]. It has been found that the nitriding improves the fatigue strength of the material and thus increases its fatigue life.

2.2.2.4.3 Plasma nitriding

Nitriding is one of the most widely used thermo-chemical methods, which produces strong and shallow case with high compressive residual stresses on the surface of steel components such as shafts, axles, gears, crankshafts, dies and tools [2.107]. However, the conventional nitriding processes based on gas or salt bath have certain limitations such as being messy and less environment-friendly and hence replaced by plasma or ion nitriding process. Plasma or ion nitriding process is preferred to the conventional techniques such as gas or liquid nitriding, since the process have the characteristics of faster nitrogen penetration, simplicity in application, cleanliness and economical aspects, as well as easier control of compound and diffusion layer formation. The requirement of lower process temperatures, shorter process periods and suppressed compound layer formation are said to be the other advantages of ion nitriding [2.108-2.110] Plasma nitriding is an advanced surface modification technology which has experienced substantial industrial development over past more than 40 years [2.111]. It is used for increasing fatigue strength, surface hardness, and corrosion or wear resistance of industrial components for a wide variety of applications. Fatigue strength of AISI 4340 steel, surface hardened via conventional gas nitriding and Ion nitriding process is demonstrated on a comparative basis in Fig.2.30 below.

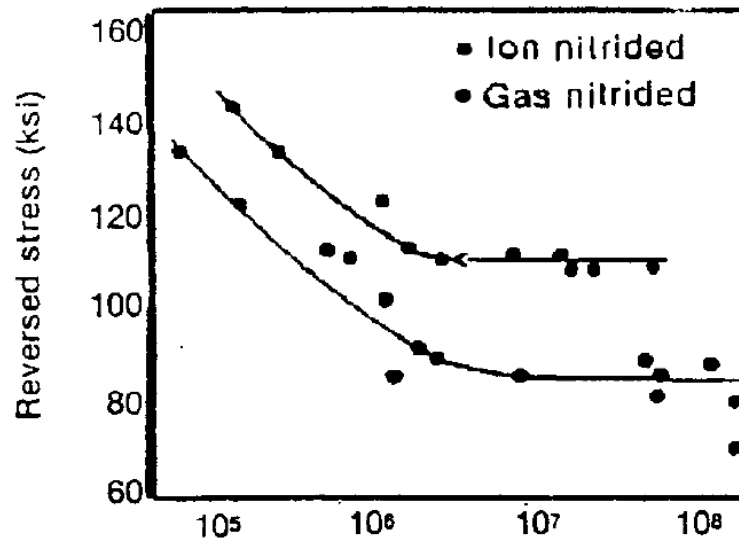


Fig. 2.30: Fatigue strength of AISI 4340 steel surface hardened via conventional gas nitriding and Ion nitriding. Ion nitriding offers greater fatigue strength than gas nitriding [2.112]

Today plasma or ion nitriding is carried out on virtually all steels and cast irons as well as refractory metals, aluminum, and sintered ferrous materials. The process is used for cutting tools, machine tools, heavy equipment, automobiles, and forging dies, injection molding dies for forming plastics, etc. [2.113-2.115].

Plasma nitriding process of surface hardening is based on glow discharge technology to introduce nascent (elemental) nitrogen into the surface of a metal part for subsequent diffusion into the workpiece. The process requires an evacuated vessel in which the workpiece becomes the cathode in a DC circuit and the vessel wall becomes the anode. Initially the vessel is evacuated to remove air/oxygen and other contaminants, and backfilled with a reactive gas such as an atmosphere containing nitrogen. A typical ionized gas mixture consists of nitrogen, hydrogen and an additive gas containing carbon, such as methane or carbon dioxide. When the electric power is turned on, the gas gets ionized, generating plasma energy. Under high vacuum, high-voltage conditions the positive ions i.e. nitrogen ions of the ionized gas strike the workpiece surface whereas the negative charges i.e. electrons are attracted towards the anode producing a glow discharge around the workpiece. This ion bombardment heats the workpiece, cleans the surface, and provides active nitrogen. Nitrogen ions combine with alloying elements such as chromium and vanadium to form a fine dispersion of alloy nitrides. Figure 2.31 gives the schematic diagram of typical plasma nitriding system.

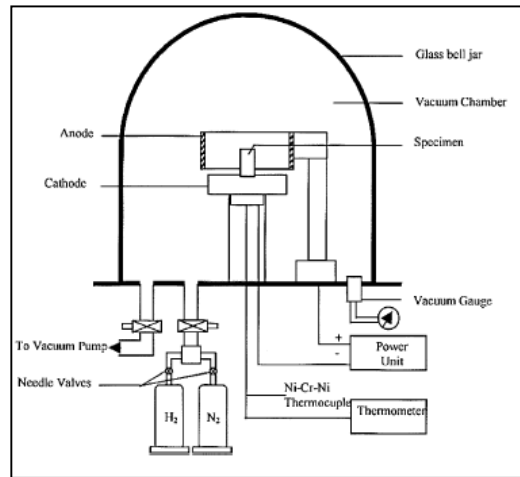


Fig. 2.31: Schematic diagram of typical plasma nitriding system [2.116]

During the ion nitriding process, the nitriding reaction not only occurs at the surface but also in the subsurface owing to the long distance diffusion of nitrogen atoms from the surface towards the core. Nitrogen diffused into the steel surface combines with alloying elements to form a fine dispersion of alloy nitrides. Not only this, the nitrogen diffusion modifies surface and near surface microstructure producing hard layers namely, compound layer and diffusion layer, as discussed earlier. The outermost layer i.e. compound layer or white layer is very thin and consists of iron nitrides ($\text{Fe}_2\text{-}_3\text{N}$ and/or, Fe_4N) [2.117, 2.118]. Beneath this layer there is diffusion layer, where the nitrogen has mainly been incorporated into the existing iron lattice as interstitial atoms or as a finely dispersed alloy precipitate. It is a relatively thick and strong diffusion zone in the subsurface of a steel component, with gradually reducing hardness and nitrogen concentration towards the core, resulting in a diffuse case-core interface [2.119]. The hardness and the depth of the diffusion layer depend mainly on the amount of nitride-former elements in the steels [2.120-2.122], the time and the temperature of the ion nitriding treatment [2.123, 2.124], the specific gas composition used in an ion nitriding system [2.125] and the initial microstructure of the material to be nitriding [2.126, 2.127] Fig 2.32 shows the role of alloy content and the nitriding time & temperature in controlling the hardness and depth of diffusion layer for a nitrided steel.

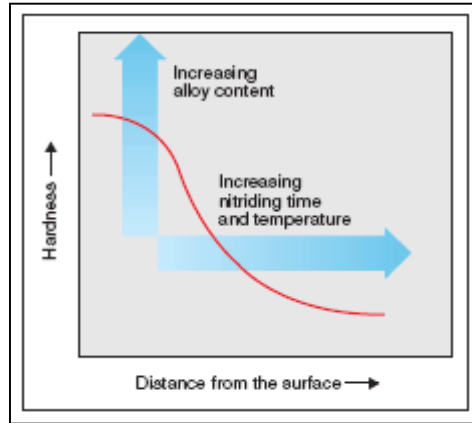


Fig. 2.32: Effect of alloy content and the nitriding time and temperature on the hardness and depth of diffusion layer for a nitrided steel [2.88]

The compound / white layer provides increased lubricity to the part. In addition to this, the compound layer being relatively inert provides increased corrosion resistance in a variety of environments. Good tribological and anticorrosion properties of nitrided steels can therefore be attributed to compound layer. The nature of the nitriding operation is such that significant amount of stresses can be imparted into the compound / white layer. Besides this, the mismatch of the thermal expansion coefficient of the phases formed within the white layer with respect to the martensite of the steel substrate also give rise to residual stresses. These residual stresses if of tensile nature, are detrimental for fatigue life of the material. Therefore, in few applications the white layer is removed from the part in a post- heat treatment machining operation. Alternatively, plasma nitriding process parameters are controlled in such a way that they create nitrided zones without a compound layer, i.e. pure diffusion layer only. On the other hand, the residual compressive stresses in the diffusion layer at the surface lead to a significant improvement in fatigue life, which can be further enhanced by combining with mechanical processes such as shot peening or surface rolling.

The effect of plasma nitriding on fatigue behaviour of various steels has been studied by several researches. In previous studies, it has been shown that the fatigue limit increases with increasing case depth and surface hardness, but the thickness of the compound layer does not influence the fatigue limit [2.128-2.130]. In addition, a few researchers investigated the relation between the process parameters of nitriding and fatigue strength [2.131-2.133].

Sule Yildiz Sirin et al [2.94, 2.100 and 2.134] investigated, in detail, the ion nitriding behaviour of quenched and tempered AISI 4340 low alloy steel under different

process parameters including time and temperature. It has been found that the ion nitriding surface treatment improves the fatigue strength and increases the fatigue limit depending on the case depth. According to this investigation, the effect of various process variables of ion nitriding for AISI 4340 steel can be summarized as under:

- The thickness of the compound layer increases with increasing treatment time and temperature. The structure of the compound layer formed during the ion nitriding of AISI 4340 steel shows a transformation from ϵ -Fe_{2,3}N nitride to γ -Fe₄N nitride with increasing treatment time and temperature. Fig. 2.33 shows the diffraction patterns obtained for ion nitrided AISI 4340 low alloy steel at different temperature and time. The X-ray analysis shows the existence of a γ -Fe₄N phase in all compound zones on the surface at all temperature and time. The compound layer consisted of γ -Fe₄N and ϵ -Fe_{2,3}N phases, and proportion of γ -Fe₄N to ϵ -Fe_{2,3}N and the thickness of this layer increased with increased time at 500 °C. The compound layer consisted of only γ -Fe₄N phase at 540 °C and the thickness of this layer increased with increased time. While γ -Fe₄N phase was forms at all temperatures and times, ϵ -Fe_{2,3}N was not formed at high temperatures.

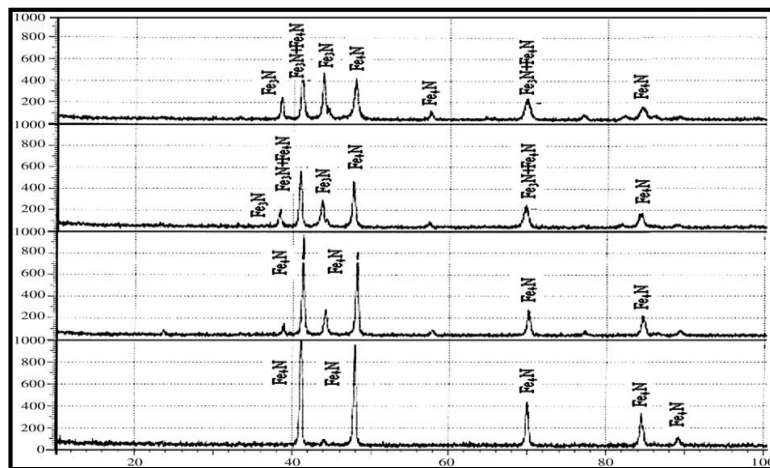


Fig. 2.33: X-Ray diffraction patterns for ion nitrided AISI 4340 low alloy steel at different temperature and time. It shows the existence of a γ -Fe₄N phase in all compound zones at all temperature and time. The compound layer consisted of γ -Fe₄N and ϵ -Fe_{2,3}N phases, and proportion of γ -Fe₄N to ϵ -Fe_{2,3}N and the thickness of this layer increased with increased time at 500 °C. [2.134]

- The case depth increases with increasing time and temperature for volume diffusion controlled growth. For this reason, the progress of case depth in ion nitriding can be expressed by a power function of process time (Fig.2.34)

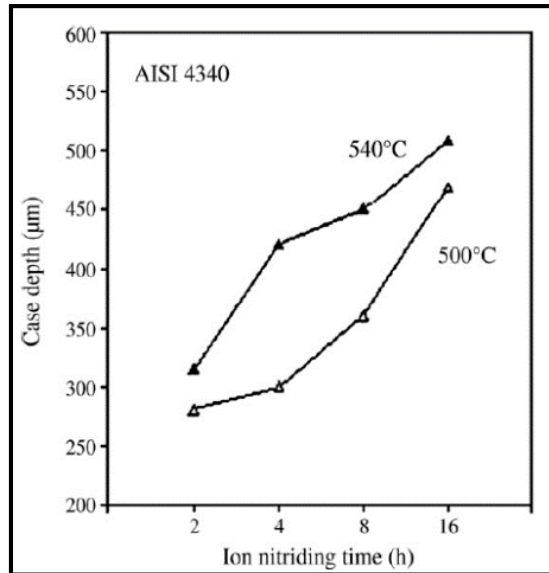


Fig. 2.34: The relationships between case depth and treatment time at 500 and 540 °C. The case depth increases with increasing time and temperature for volume diffusion controlled growth [2.134]

- The surface hardness increases with increasing time and temperature of ion nitriding treatment as shown in following figure.

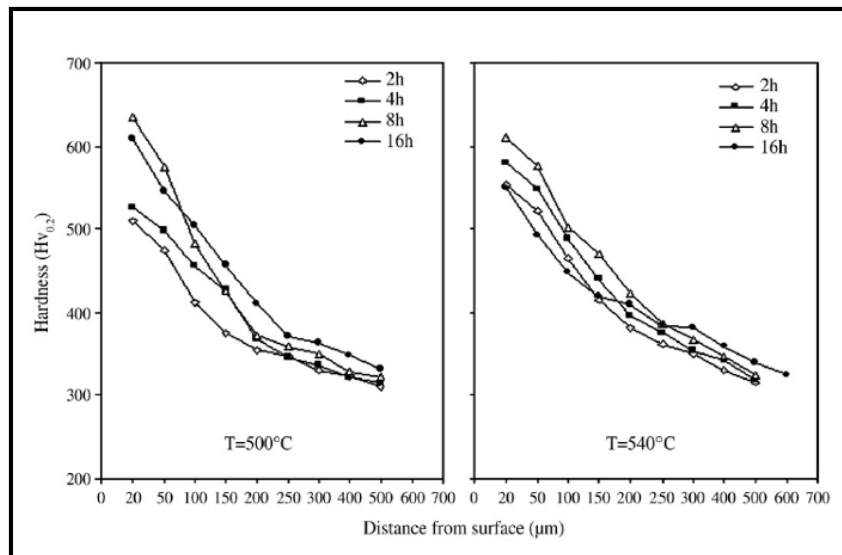


Fig. 2.35: Effect of plasma nitriding temperature and time on surface hardness of AISI4340 steel. The surface hardness increases with increasing time and temperature of ion nitriding treatment [2.134]

- Up to 91% improvement in fatigue strength of the steel has been attained by ion nitriding. A linear relationship is found to exist between fatigue strength of steel and case depth (Fig. 2.36)

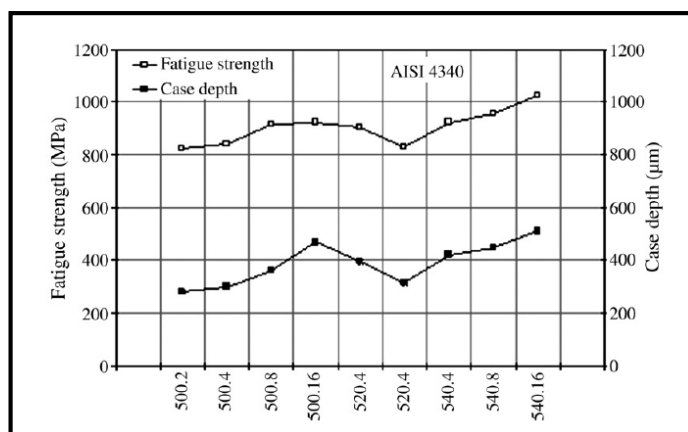


Fig. 2.36: Relationship between fatigue strength of steel and case depth for AISI4340 steel. A linear relationship is found to exist between fatigue strength of steel and case depth [2.134]

Sule Yildiz Sirin and co-workers [2.134], attribute the improvement in fatigue behaviour to alterations of the surface properties and some of the other factors, as discussed below. First of all, the formation of precipitate particles in nitrided layer can hinder dislocation motion and, therefore, slip band penetration through the nitrided layer. A diffusion layer, which is formed during ion nitriding process, causes compressive residual stresses on or near the surface of the component, as well as low tensile residual stress in the core. Both increased residual stress and surface hardness result in improvements in the fatigue life because the thin, hard layer prevents plastic flow. Therefore, the slip bands can only be activated by very high stresses in this region. This means that plastic deformation, which is the source of crack initiation, probably appears in the subsurface. The suppression of slip band formation at the surface delays crack initiation and propagation, thus contributes in improving the fatigue life [2.135].

A. Celik and S. Karadeniz studied the influence of plasma nitriding on the fatigue behaviour of AISI 4140 low-alloy steel under varying process conditions of temperature (500-600 °C), time (1-12 h), heat treatment before ion nitriding (quenched and tempered, normalized) and gas mixture (50% H₂-50% N₂) [2.136]. A rotating bending fatigue machine was used to determine the fatigue strength. It was found that the plasma nitriding improves the fatigue strength and increases the fatigue limit depending on the surface hardness of the case depth. This study has also demonstrated that the fatigue strength of material depends on the surface hardness of the case depth, because the origin of fatigue cracks moves into the core owing to the high surface hardness of the specimens, i.e., if the material has a high surface hardness, fatigue

cracks will tend to initiate in the subsurface (below the case depth); however, if the material has a low surface hardness, fatigue cracks initiate and propagate in the surface.

Celik and Karadeniz examined the compound layer formed in AISI 4140 steel after ion nitriding at temperatures of 500, 550 and 600 °C for various times in a 50% N₂-50% H₂ gas mixture [2.137]. It was observed that the thickness of the compound layer increases with increasing time at 500 and 550 °C; however, it begins to decrease with increasing time at 600 °C.

Kenan Genel et. al. [2.138] investigated the effect of case depth on fatigue performance of AISI 4140 low alloy steel that had been ion nitrided at 748 K for 1, 3, 8 and 16 h. The investigation revealed that a remarkable improvement (as much as 50%) in fatigue life can be obtained by the application of ion nitriding as shown in Fig.2.37.

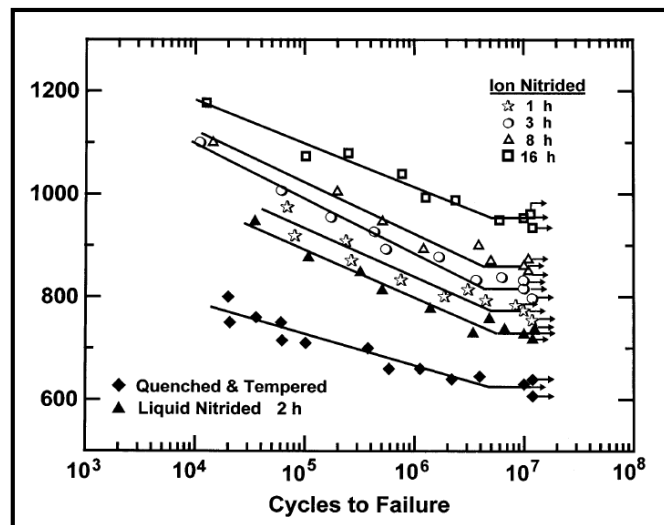


Fig. 2.37: Fatigue curves of heat treated, liquid and ion nitrided AISI 4140 steel for various process times. A remarkable improvement (as much as 50%) in fatigue life can be obtained by the application of ion nitriding [2.138]

In this study, a series of fatigue tests on ion nitrided AISI 4140 steel with different case depths were conducted and efforts were made to construct empirical relationships between relative case depth and fatigue limit of ion nitrided steel. Since the section size is one of the most important factors determining the fatigue performance of machine components, some dimensionless parameters were defined to express the proportion of nitrided case zone in the whole cross-section such as, relative case area A_R , which is defined as the ratio of case area to core area and the ratio of specimen diameter to core

diameter $D:(D-2t)$ for round specimens. Alternatively, the ratio of case depth to specimen diameter $t:D$ can also be used for simplicity. A linear relationship was obtained between fatigue strength of the steel and relative case depth of specimens, which is defined as the ratio of case depth to the diameter of specimen, up to the value of 0.08 for relative case depth. It was found that compressive residual stresses on the surface of ion nitrided specimens increase with increasing case depth, up to the value 0.075 of relative case depth, with decreasing rate. Exceeding this critical limit of relative case depth, there is a tendency of reduction in compressive residual stress on the surface as demonstrated in Fig. 2.38. It is therefore recommended that, the relative case depth $t:D$ of ion nitride machine components should not exceed 0.075 in industrial applications, when the tendency of reduction in compressive residual stress and the probability in easy cracking behaviour of thick brittle case, as well as the economical aspects of the process are taken into account.

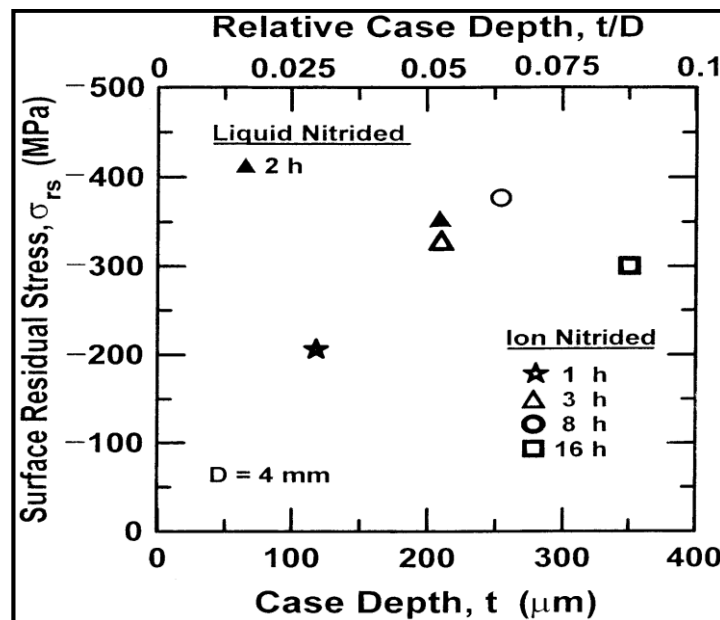


Fig. 2.38: Variation in compressive residual stress on the surfaces of specimens with nitriding time and case depth, respectively [2.138]

The effect of relative case depth $t:D$ and the parameter $D:(D-2t)$ on the fatigue strength of ion nitrided AISI 4140 steel is demonstrated in following Fig.2.39 [2.138].

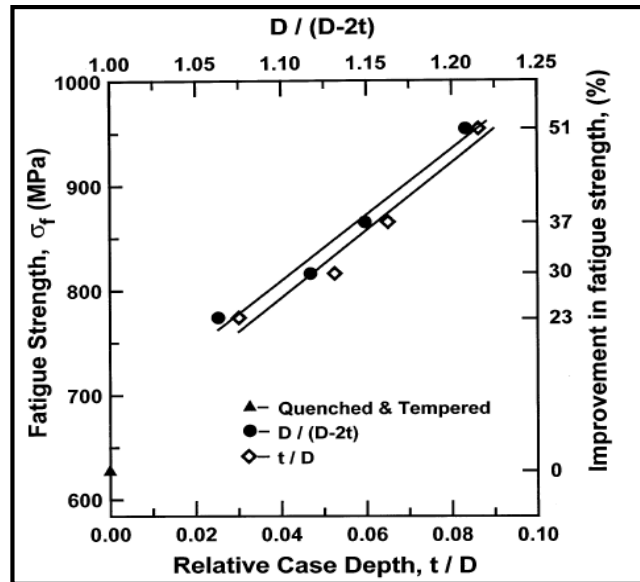


Fig.2.39: Effect of relative case depth t/D and the parameter $D:(D-2t)$ on the fatigue strength of ion nitrided AISI 4140 steel [2.138].

Similar studies have also been carried out by Sule Sirin and co-workers [2.100] to examine of ion nitriding on fatigue behaviour of AISI 4340 steel under different process parameters including time and temperature as displayed in Fig.2.40. It was found that the ion nitriding surface treatment improves the fatigue strength and increases the fatigue limit depending on the case depth. Up to 91% improvement in fatigue strength of the steel has been attained by ion nitriding. A linear relationship was obtained between fatigue strength of steel and case depth (Fig. 2.41).

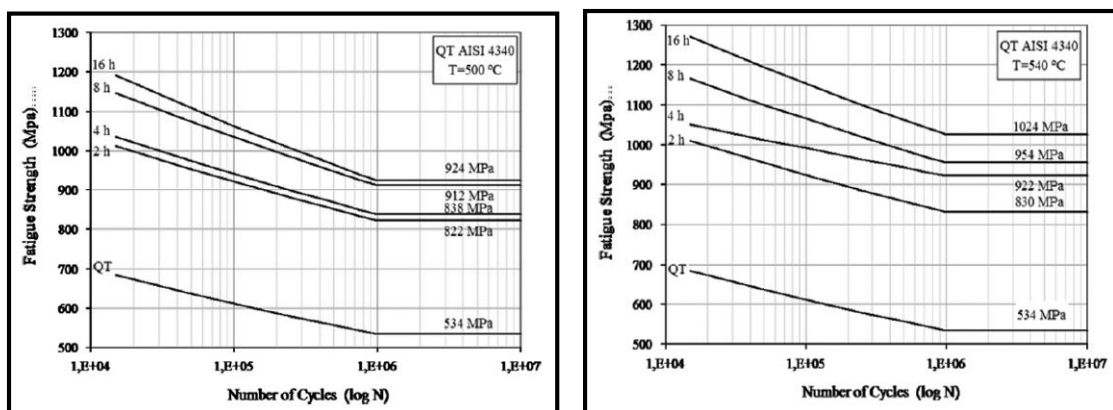


Fig. 2.40: Fatigue curves of QT AISI4340 steel ion-nitrided at 500 °C and 540 °C for 2, 4, 8 and 16 h. [2.100]

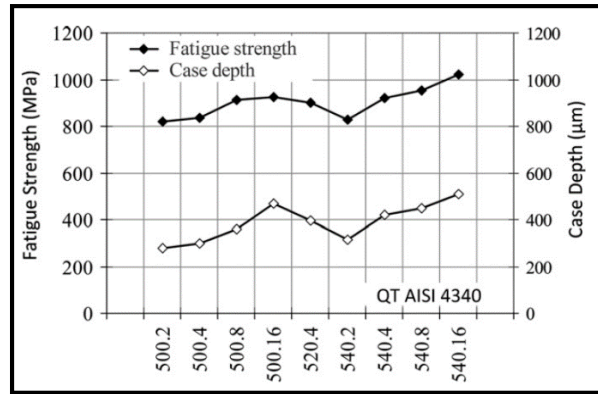


Fig.2.41: Relationship between case depth and fatigue strength of ion-nitrided QT AISI 4340 steel. The ion nitriding surface treatment improves the fatigue strength and increases the fatigue limit depending on the case depth. [2.100]

2.2.3 Role of residual stresses in compound layer on fatigue life of steels:

Residual stresses are self-equilibrating stresses existing in materials at uniform temperature and without external loading and are often found to arise in materials during processing steps, such as, electroplating, heat treatment or machining. The origins of residual stresses have been ascribed to compositional changes, thermal effects, lattice defects and the formation of precipitates. One of the most important and widely used thermochemical surface treatments to bring about a beneficial state of residual stress is nitriding. The residual stress in the nitride layer on the surface has been a subject of research since long [2.139-2.142].

The process of nitriding involves:

- (i) The compositional gradient of nitrogen,
- (ii) The precipitation of nitrides (γ' -nitride in original ϵ -nitride) which have a larger atomic volume of metal than the matrix,
- (iii) Misfit between γ' - and ϵ -nitride in two phase layers,
- (iv) Thermal stresses,
- (v) Formation of nitrogen filled pores.

Nitriding leads to the generation of pronounced residual internal stresses in the diffusion zone. There are a number of reasons for this [2.143]:

- (i) Thermal stresses due to thermal expansion or contraction of a homogeneous material in a temperature gradient field,
- (ii) Difference in thermal expansion coefficients of the various phases in a multiphase material,

- (iii) Density changes due to phase transformations in the metal,
- (iv) Growth stresses of reaction products formed on the surface or as precipitates, and
- (v) Chemical compositional gradients below the surface.

In short, macro-stresses build up within the compound layer during growth due to a compositional misfit within the layers caused by the concentration gradient and, after growth, due to a thermal misfit between the layer phases and the substrate, viz. different coefficients of thermal expansion of the different phases. The main cause for residual stress in the metal phase is the chemical gradient of nitrogen from the surface inwards.

The residual macro-stresses arising during nitriding due to the difference in specific volume between the matrix and the nitrides can be described in a simplified way as follows [2.144] Consider first an un-nitrided specimen (See Fig. 2.42(a)), during nitriding nitrogen is absorbed through the surface and diffuses through the sample. Nitrogen combines with the nitride-forming elements and subsequently nitrides precipitate. As there is a difference in specific volume between the matrix and the nitrides, the nitrided layer would tend to expand as shown in Fig. 2.42(b). However, the nitrided layer is attached to the sample, so it cannot expand freely; the matrix counterbalances the expansion by means of compressive stresses, which develop in the nitrided layer. At the same time, to maintain the mechanical equilibrium of the nitrided specimen, small tensile stresses develop in the un-nitrided core as per Fig. 2.42(c).

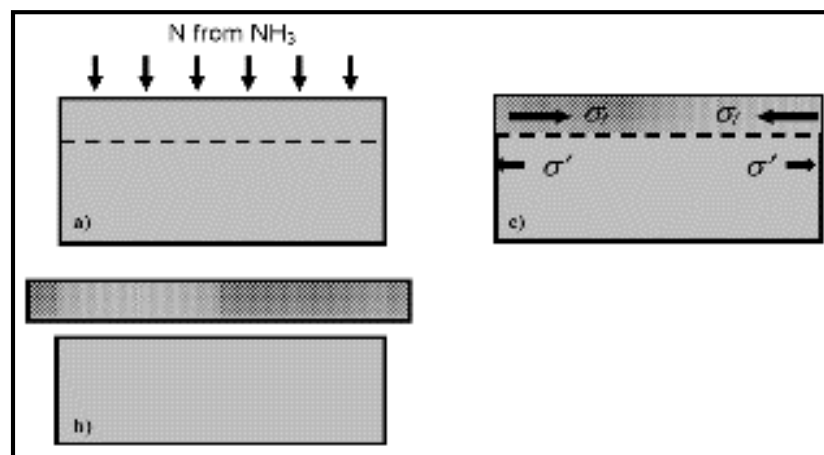


Fig. 2.42: Schematic representation of the development of residual macrostresses nitrided iron-based alloys. Stresses developed are compressive in the surface while tensile in sub-surface. [2.144]

Fig. 2.43 gives a schematic representation of the precipitation of a coherent nitride particle and the corresponding occurrence of strain fields in the surrounding ferrite matrix leading to hardening effect.

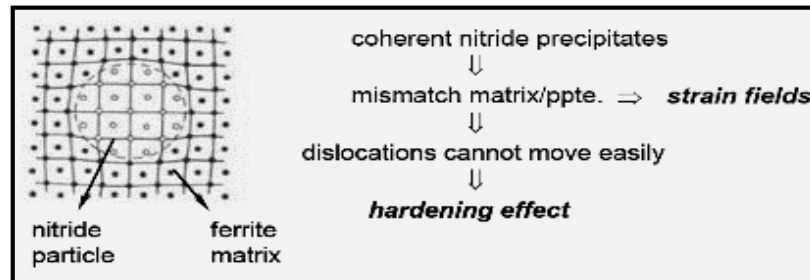


Fig. 2.43: Schematic representation of the precipitation of a coherent nitride particle and the corresponding occurrence of strain fields in the surrounding ferrite matrix leading to hardening effect

Finally a very significant cause is the interaction between the compound layer and the metal matrix due to different atomic volumes of the metal and different thermal expansion coefficients. The interaction should give a tensile stress contribution to the metal surface zone and a strong compressive stress contribution to the compound layer.

A typical residual stress depth profile for smooth plasma nitrided specimen is shown in Fig. 2.44. The profile indicates that as the depth of nitriding increases the residual stress decreases.

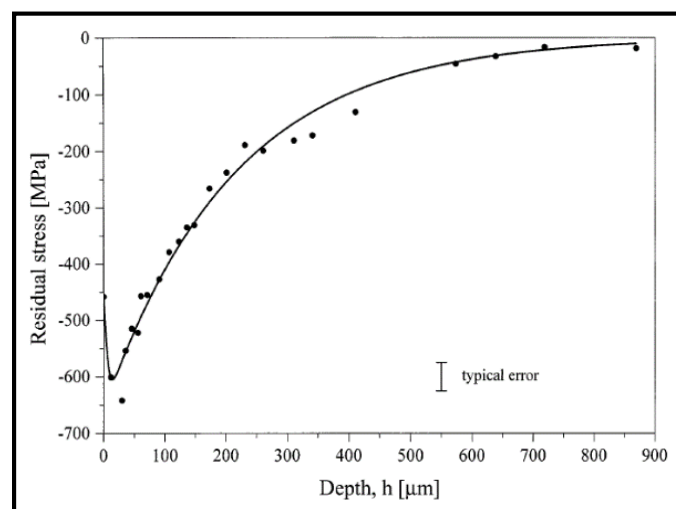


Figure 2.44: A typical residual stress depth profile for smooth plasma nitrided specimen indicates that as the depth of nitriding increases the residual stress decreases [2.145]

As discussed earlier, the residual stresses have a crucial influence on the (mechanical) properties of nitrided specimens. This holds good particularly for the fatigue properties: the presence of compressive residual stresses parallel to the surface in the surface-adjacent regions of the specimen can prevent crack initiation and crack growth.

2.3 Finite Element Analysis

Finite Element Analysis or Method (FEA or FEM) is a tool used for solving engineering problems through modeling and simulation. FEA is extensively used for stress and fatigue analysis of dynamically loaded components [2.151-2.156].

Components subjected to surface treatments are most likely to initiate fatigue cracks at surface. Hence, stress pattern developed at and near surface are required to be established using simulation methods. Usually the surface treatments generate residual stresses in the surface [2.31-2.35, 2.77]. FEM tool is used to determine residual stresses of components subjected to thermal, thermo-mechanical and mechanical treatments [2.155].

At the same time, state of stress in the surface layer, while it is subjected to loading, will change the stress pattern already existing due to residual stresses [2.92, 2.142, 2.148-2.150].

However, for determining stress state using FEA, availability of precise data on mechanical properties of phases present in the surface is important. Also, results of such analysis done have to be validated before it is used for actual application.

Compound (white) layers in the plasma nitrided components comprise of various types of nitrides (ϵ -nitrides & γ' -nitrides) which have different mechanical properties. Hence, the response of such layers to the loading will vary depending on the phases present. Plasma nitrided components have not been studied for state of stress developed in the compound layers of varying phases. Using the property related data available on various nitrides [2.142 & 2.147] it is possible to determine the effective state of stress in the compound layer and then correlate with the experimental results of fatigue testing.